

2HDM interpretations of the CMS diphoton excess at 95 GeV

Duarte Azevedo^{1,2*}, Thomas Biekötter^{1†}, P.M. Ferreira^{3,4‡}

¹*Institute for Theoretical Physics, Karlsruhe Institute of Technology,
Wolfgang-Gaede-Str. 1, 76128 Karlsruhe, Germany*

²*Institute for Astroparticle Physics, Karlsruhe Institute of Technology,
Hermann-von-Helmholtz-Platz 1, 76344 Eggenstein-Leopoldshafen, Germany*

³*Centro de Física Teórica e Computacional, Faculdade de Ciências,
Universidade de Lisboa, Campo Grande, Edifício C8 1749-016 Lisboa, Portugal*

⁴*ISEL - Instituto Superior de Engenharia de Lisboa,
Instituto Politécnico de Lisboa 1959-007 Lisboa, Portugal*

Abstract

In both Run 1 and Run 2 of the LHC, the CMS collaboration has observed an excess of events in the searches for low-mass Higgs bosons in the diphoton final state at a mass of about 95 GeV. After a recent update of the experimental analysis, in which the full Run 2 data collected at 13 TeV has been included and an improved experimental calibration has been applied, the local significance of the excess amounts to 2.9σ . The presence of this diphoton excess is especially interesting in view of a further excess observed by CMS in ditau final states at a comparable mass and similar local significance. Moreover, an excess of events with about 2σ local significance and consistent with a mass of 95 GeV was observed in LEP searches for a Higgs boson decaying to pairs of bottom quarks. We interpret the CMS diphoton excess in combination with the ditau excess in terms of a pseudoscalar resonance in the CP-conserving two-Higgs-doublet model (2HDM). Furthermore, we discuss the possibility that, if CP-violation is taken into account, a CP-mixed scalar state can in addition describe the LEP result, thus accommodating all three excesses simultaneously. We find that the region of parameter space where both the CMS diphoton and ditau excesses can be fitted is in tension with current constraints from the flavour sector, potentially calling for other new-physics contributions to flavour-physics observables, most notably $b \rightarrow s\gamma$ transitions. We also comment on the compatibility with the recent ATLAS di-photon searches.

*E-mail: duarte.azevedo@kit.edu

†E-mail: thomas.biekoetter@kit.edu

‡E-mail: pmmferreira@fc.ul.pt

Contents

1	Introduction	1
2	The Model	2
2.1	The real 2HDM	4
2.2	The complex 2HDM	5
3	Possible indications for a new scalar at 95 GeV	7
3.1	The CMS diphoton excess	7
3.2	The CMS ditau excess	9
3.3	The LEP excess strikes back	9
3.4	Summary of possible signals	11
3.5	Additional experimental findings regarding a possible state at 95 GeV	11
4	2HDM scenarios to reproduce the 95 GeV data	12
4.1	Parameter scans, theoretical and experimental constraints	12
4.2	Real 2HDM type I – $m_A = 95$ GeV	13
4.2.1	Properties of $h = h_{125}$	16
4.2.2	Properties of the other BSM states	17
4.2.3	Flavour-physics constraints	19
4.3	Real 2HDM type I – $m_H = 95$ GeV	21
4.4	Real 2HDM type LS	21
4.5	Complex 2HDM – $m_{h_1} = 95$ GeV, $m_{h_2} = 125$ GeV, $m_{h_3} > 130$ GeV	22
4.5.1	Properties of $h_2 = h_{125}$	24
4.5.2	Properties of the other BSM states	26
4.5.3	Flavour-physics constraints	27
4.5.4	EDM constraints	28
4.6	Complex 2HDM – $m_{h_1} = 95$ GeV, $m_{h_2} = 125$ GeV, $m_{h_3} < 120$ GeV	29
4.7	Complex 2HDM – Lepton-specific	30
5	Conclusions	30

1 Introduction

After the discovery of a Higgs boson at the Large Hadron Collider (LHC) by the ATLAS and CMS experiments [1, 2], a prime goal of the current LHC programme is to investigate whether the detected Higgs boson is the only fundamental scalar particle, according to the predictions of the Standard Model (SM), or whether it is part of a Beyond the Standard Model (BSM) theory with extended Higgs sectors and additional Higgs bosons. So far no new scalars were found at the LHC and no conclusive indirect hints of new physics have been reported. With increasing precision in the measurements of the Higgs couplings to fermions and gauge bosons, the parameter space of BSM models has been continuously reduced, but the present experimental uncertainties leave room for a BSM interpretation of the detected Higgs boson.

Many BSM theories incorporate extended Higgs sectors with additional scalar particles. In particular, the presence of additional Higgs bosons with masses below 125 GeV is not excluded if their couplings are suppressed compared to the couplings of a SM Higgs boson. It could very well be that these additional Higgs bosons are within the reach of the LHC, and with

large enough couplings these scalars would have been produced in small numbers in past runs. Thus, an intriguing question is whether there could be hints for an additional Higgs boson in the currently existing searches in the form of yet non-significant excesses over the background expectation.

In this paper, we will focus on a series of results presented by the CMS collaboration on searches for a scalar particle produced through gluon fusion at the LHC. These show excesses at the level of 3σ local significance in the diphoton [3–5] and ditau [6] final states, compatible with a scalar resonance with a mass around 95 GeV. Moreover, an additional mild excess of 2σ local significance consistent with a mass of 95 GeV was observed at the Large Electron-Positron (LEP) collider assuming the decay of a scalar resonance to bottom-quark pairs [7]. The diphoton excess in particular has been the subject of many recent works (see, e.g. Refs. [8–16], where in Refs. [17–22] also the ditau excess observed by CMS was considered, and Refs. [21, 23] are based on the most recent CMS diphoton search including the full Run 2 dataset). We will interpret these excesses in the two-Higgs-doublet model (2HDM) in its charge-parity (CP)-conserving and explicitly CP-violating realization.

Shortly after the update on CMS’s low-mass diphoton searches, ATLAS has also published its result for the full Run 2 search for low-mass Higgs bosons decaying into diphotons [24]. In the “model-dependent” ATLAS analysis, which has very similar experimental sensitivity to the CMS analysis, the most pronounced excess is observed for a mass of 95.4 GeV, with 1.7σ local significance. The excess is not as pronounced as the ones reported by CMS, but the mass value is in very good agreement, and a possible combination of the ATLAS result with the CMS results would give rise to slightly smaller signal rates. We therefore argue that even the small upwards fluctuation seen at ATLAS cannot exclude the signal interpretation of the CMS diphoton excesses. In this paper, we will solely interpret the CMS excesses but the results can be easily extended assuming a somewhat smaller ATLAS+CMS combined signal strength. We also wish, with this work, to show how easily a low-mass diphoton excess for masses of order ~ 95 GeV can be fitted in the 2HDM – if the current CMS excesses are disproven with future observations but others appear in future data, the 2HDM should be considered as a possible immediate explanation.

The paper is divided as follows: Sect. 2 introduces the model and its CP realizations. The experimental searches that showed the excesses are discussed in detail in Sect. 3, where we also discuss the compatibility of the excesses with corresponding ATLAS results. Afterwards, the pertinent scenarios that accommodate the excesses in the 2HDM are analysed in Sect. 4, and the relevant experimental constraints are reviewed and their compatibility considered. Further possibilities that might enable a distinction between the realizations put forward here and other model interpretations of the excesses published in the past are also discussed. Finally, we summarize and conclude in Sect. 5.

2 The Model

The 2HDM is one of the simplest extensions of the Standard Model of particle physics. It was introduced in 1973 by T.D. Lee [25] to allow for extra sources of CP violation beyond the CKM matrix. The model has the same gauge symmetries and fermionic and vector gauge content of the SM but with two $SU(2)$ hypercharge $Y = 1$ Higgs doublets. Such a minimalist extension of the SM allows for a very rich phenomenology, including the existence of three neutral scalars and a pair of charged scalars; violation of the CP symmetry, both explicit or spontaneous; dark matter candidates; non-trivial contributions to flavour physics, via flavour-changing neutral currents

	u -type	d -type	charged leptons
Type I	Φ_2	Φ_2	Φ_2
Type II	Φ_2	Φ_1	Φ_1
Lepton-specific	Φ_2	Φ_2	Φ_1
Flipped	Φ_2	Φ_1	Φ_2

Table 1: The four models of the \mathbb{Z}_2 -symmetric 2HDM. Each group of fermions of the same electric charge is made to couple to a single doublet, preventing tree-level FCNC interactions.

(FCNCs). Moreover, the presence of a second Higgs doublet is motivated by supersymmetric extensions of the SM [26], or by models addressing the strong CP-problem of QCD [27, 28]. For a review of the 2HDM, see for instance Ref. [29].

The most general scalar potential of the 2HDM has 11 independent real parameters [30], as opposed to the SM potential, which depends only on 2 real parameters. Furthermore, the fermion sector of the most general 2HDM has twice the number of complex 3×3 Yukawa matrices than the SM, which substantially curtails the 2HDM predictive power. It is therefore customary to impose discrete symmetries on the 2HDM Lagrangian. For instance, given that FCNC are strongly constrained by experimental results, one can consider the invariance over a \mathbb{Z}_2 transformation on the doublets [31, 32], $\Phi_1 \rightarrow \Phi_1$ and $\Phi_2 \rightarrow -\Phi_2$. When extended to the Yukawa sector, this symmetry forces each set of fermions of the same electric charge to couple to a single doublet, instead of both. As a consequence, the model is free of tree-level FCNC mediated by scalars. There are four possibilities to extend the \mathbb{Z}_2 symmetry to the Yukawa sector, depending on how the up-type quarks, down-type quarks and charged leptons transform under this symmetry.¹ Per convention the mass of the up-type quarks is always considered to be proportional to v_2 (the vacuum expectation value of Φ_2), which leaves the four possibilities shown in Tab. 1. In Type I, all fermions couple to (and gain mass from) the same doublet, Φ_2 , whereas in Type II down-type quarks and charged masses couple to Φ_1 instead, a construction familiar from supersymmetric extensions of the SM. These choices for fermion interactions have substantial impact on the phenomenology of each of the four models [33]. In particular, often the most stringent constraint from the flavour sector on these models stems from experimental data on the decay $b \rightarrow s\gamma$, NLO analytical expressions for which may be found in Ref. [34]. For models of Type II and Flipped, the constraints from $b \rightarrow s\gamma$ transitions force $\tan\beta \gtrsim 1$ and the charged Higgs-boson mass to be pushed in to the hundreds of GeV. For models of Type I and Lepton-specific (LS), there is a lower bound on $\tan\beta$ depending on the value of the charged scalar mass. Since in this work we will be interested in reproducing the phenomenology of a particle with a mass of about 95 GeV, models Type II and Flipped are therefore ruled out *a priori*: a mass of the charged Higgs boson several hundreds of GeV larger than the EW scale in combination with at least two neutral scalar states at and below 125 GeV is incompatible with constraints from electroweak precision measurements (in the form of bounds on the oblique parameters S , T and U) and theoretical constraints from perturbativity.

If the 2HDM \mathbb{Z}_2 symmetry is spontaneously broken, the scalar potential does not allow for a *decoupling limit*, *i.e.* the possibility of having a SM-like Higgs boson with mass approximately 125 GeV and all the other extra scalars being as heavy as desired, in particular, to elude current LHC experimental bounds [35]. To contemplate the possibility of a decoupling limit, then, one

¹In fact there will be more possibilities if one considers Dirac mass terms for neutrinos, which we will not do in this paper.

introduces a dimension-2 *soft breaking* term in the potential, m_{12}^2 . The scalar potential becomes

$$\begin{aligned}
V = & m_{11}^2 |\Phi_1|^2 + m_{22}^2 |\Phi_2|^2 - m_{12}^2 \left(\Phi_1^\dagger \Phi_2 + \text{h.c.} \right) + \frac{\lambda_1}{2} (\Phi_1^\dagger \Phi_1)^2 + \frac{\lambda_2}{2} (\Phi_2^\dagger \Phi_2)^2 \\
& + \lambda_3 (\Phi_1^\dagger \Phi_1) (\Phi_2^\dagger \Phi_2) + \lambda_4 (\Phi_1^\dagger \Phi_2) (\Phi_2^\dagger \Phi_1) + \frac{\lambda_5}{2} \left[(\Phi_1^\dagger \Phi_2)^2 + \text{h.c.} \right] , \quad (2.1)
\end{aligned}$$

with all parameters real. The introduction of m_{12}^2 does not lead to any extra infinities in high order calculations. Additionally, the scalar potential explicitly preserves CP, though spontaneous CP breaking may occur. On the other hand, if m_{12}^2 and λ_5 are complex with unrelated phases the CP symmetry is explicitly broken. In this paper, we will be studying both possibilities. We refer to the former as the *real* 2HDM (R2HDM), and to the latter as the *complex* 2HDM (C2HDM) [36–44]. Another argument in favour of soft breaking the \mathbb{Z}_2 symmetry is to avoid the possibility of domain walls forming [45].

Regardless of soft breaking, the potential of eq. Eq. (2.1) is subject to a series of basic constraints: (i) it must be *bounded from below*, which means that, regardless of how large the fields become, it can never tend to minus infinity; (ii) it must respect *unitarity*, so that a perturbation theory approach of quantum amplitudes remains valid; (iii) and it must satisfy *electroweak precision constraints*, which stem, among others, from precise measurements of the masses of the W and Z bosons. Constraints (i) and (ii) impose limits on the quartic couplings of the potential (see [46–48] and [49, 50], respectively) and constraint (iii) limits mass splittings on the scalars of the model [51]. All of these bounds are implemented in the numerical scans we will present, being a part of the code `ScannerS` [52]. In addition, we confront the parameter points with the cross section limits from searches for additional Higgs bosons at LEP and the LHC and with the LHC cross section measurements of the detected Higgs boson at 125 GeV using the code `HiggsTools v.1` [53] (which incorporates the codes `HiggsBounds` [54–57] and `HiggsSignals` [58–60]). More details on the applied constraints and the computation of the respective theory predictions can be found in Sect. 4.1.

2.1 The real 2HDM

Though spontaneous CP breaking is possible with real m_{12}^2 , in the current work we are interested in a vacuum which preserves CP. Therefore, we will only consider minima for which the doublets acquire neutral and real vacuum expectation values (vevs), $\langle \Phi_1 \rangle = v_1/\sqrt{2}$ and $\langle \Phi_2 \rangle = v_2/\sqrt{2}$, such that $v_1^2 + v_2^2 = v^2 = 246^2$ GeV². Without loss of generality, we can take both vevs to be positive. The scalar spectrum of this model yields a pair of charged scalar particles H^\pm and three neutral ones - two CP-even eigenstates, h and H , and a CP-odd one, the pseudoscalar A . m_h and m_H are the eigenvalues of a 2×2 matrix, diagonalized by an angle α , taken, without loss of generality, to vary between $-\pi/2$ and $\pi/2$. Another angle is defined by the ratio of the vevs, $\tan \beta = v_2/v_1$. The importance of α and β stems from the fact that the strength of most of the couplings of the scalars may, in this model, be expressed as functions of those two angles. For instance, the couplings of h and H to the electroweak gauge bosons $V = W, Z$ are given by

$$g_{(h/H)VV} = C_{(h/H)} g_{hVV}^{SM} \quad , \quad C_h = \sin(\beta - \alpha) \quad , \quad C_H = \cos(\beta - \alpha) \quad (2.2)$$

where g_{hVV}^{SM} is the coupling between the SM Higgs boson and the electroweak gauge bosons. Notice how, due to the electroweak gauge symmetry, the coupling modifiers obey a sum rule, $g_{hVV}^2 + g_{HVV}^2 = (g_{hVV}^{SM})^2$. The pseudoscalar, A , will not have such couplings to W 's or Z 's.

As for the Yukawa Lagrangian, it is given by

$$\begin{aligned} \mathcal{L}_{\text{Yukawa}} = & - \sum_{f=u,d,\ell} \frac{m_f}{v} \left(\xi_h^f \bar{f} f h + \xi_H^f \bar{f} f H - i \xi_A^f \bar{f} \gamma_5 f A \right) \\ & - \left\{ \frac{\sqrt{2} V_{ud}}{v} \bar{u} \left(m_u \xi_A^u P_L + m_d \xi_A^d P_R \right) d H^+ + \frac{\sqrt{2} m_\ell \xi_A^\ell}{v} \bar{\nu}_L \ell_R H^+ + \text{H.c.} \right\} \end{aligned} \quad (2.3)$$

where m_x is the mass of fermion x , u and d generic up and down-type quarks respectively, and V_{ud} the corresponding CKM matrix element. The coupling modifiers ξ are functions of α and β alone. In model Type I, which will be the almost exclusive focus of this paper, they are given by

$$\begin{aligned} \xi_h^f &= \sin(\beta - \alpha) + \frac{1}{\tan \beta} \cos(\beta - \alpha), \\ \xi_H^f &= \cos(\beta - \alpha) - \frac{1}{\tan \beta} \sin(\beta - \alpha), \\ \xi_A^u = -\xi_A^d &= \frac{1}{\tan \beta}. \end{aligned} \quad (2.4)$$

In the *alignment limit*, where h has almost SM-like interactions, $\cos(\beta - \alpha) \simeq 0$, and we see that the magnitude of the coupling modifiers for H and A grow with $1/\tan \beta$. Likewise, the strengths of the couplings of the charged scalar increase for lower values of $\tan \beta$. As we will see in Section 4, the use of these coupling modifiers allows one to considerably simplify the analysis of the phenomenology of the model. For the LS model, which we will also briefly discuss in the numerical analysis, the coupling modifiers of scalars to charged leptons are different than those of quarks, namely

$$\begin{aligned} \xi_h^l &= \sin(\beta - \alpha) - \tan \beta \cos(\beta - \alpha), \\ \xi_H^l &= \cos(\beta - \alpha) + \tan \beta \sin(\beta - \alpha), \\ \xi_A^l &= \tan \beta, \end{aligned} \quad (2.5)$$

now the coupling modifiers for H , A and H^\pm grow with $\tan \beta$. The alignment limit has the same definition as in Type I.

For future reference, we will use the following set of input parameters to describe a R2HDM parameter point

$$m_h, \quad m_H, \quad m_A, \quad m_{H^\pm}, \quad C_H, \quad \tan \beta, \quad m_{12}^2, \quad v, \quad (2.6)$$

where $m_h = 125$ GeV and $v = v_{\text{EW}} = 246$ GeV are fixed to the known values.

2.2 The complex 2HDM

If both m_{12}^2 and λ_5 are complex with unrelated phases, then the 2HDM scalar potential explicitly breaks the CP symmetry. It will not be possible to rotate all of the phases away through field re-definitions, even though the vevs can be set to be real and positive without loss of generality. Thus, like before, we have $\langle \Phi_1 \rangle = v_1/\sqrt{2}$ and $\langle \Phi_2 \rangle = v_2/\sqrt{2}$, with $v_1^2 + v_2^2 = v^2 = 246^2$ GeV². The now complex soft \mathbb{Z}_2 -breaking term, m_{12}^2 , does not spoil the absence of tree-level FCNC.

In this section we review the basic notation of the C2HDM, referring the reader to Ref. [61] for more details. As in the real 2HDM, the scalar spectrum is composed of a pair of charged

scalars and three neutral ones. However, since the CP-symmetry is explicitly broken, those three neutral states are not CP-even or CP-odd, rather they have indefinite CP quantum numbers, since they result from the mixing of real and imaginary components of the neutral fields of the doublets. The three neutral mass eigenstates h_i ($i = 1, 2, 3$) are found to be the eigenvalues of a 3×3 real and symmetric mass matrix, diagonalized by an orthogonal rotation matrix R_{ij} , parameterized in terms of three angles α_1, α_2 and α_3 as [44]

$$R = \begin{pmatrix} c_1 c_2 & s_1 c_2 & s_2 \\ -(c_1 s_2 s_3 + s_1 c_3) & c_1 c_3 - s_1 s_2 s_3 & c_2 s_3 \\ -c_1 s_2 c_3 + s_1 s_3 & -(c_1 s_3 + s_1 s_2 c_3) & c_2 c_3 \end{pmatrix}, \quad (2.7)$$

where we define $s_i \equiv \sin \alpha_i$, $c_i \equiv \cos \alpha_i$. Without loss of generality, we can choose [39]

$$-\pi/2 < \alpha_1 \leq \pi/2, \quad -\pi/2 < \alpha_2 \leq \pi/2, \quad 0 \leq \alpha_3 \leq \pi/2. \quad (2.8)$$

The angle α_2 controls the mixture between different CP eigenstates. In particular, it may be shown that if $s_2 = 0$ the scalar h_1 is a pure scalar; but if $|s_2| = 1$ then h_1 would be a pure pseudoscalar.

The three α angles and β appear frequently in studies of C2HDM phenomenology.² For instance, there is a relation between the masses m_{h_i} of the neutral scalars and these angles, to wit

$$m_{h_3}^2 = \frac{m_{h_1}^2 R_{13}(R_{12} \tan \beta - R_{11}) + m_{h_2}^2 R_{23}(R_{22} \tan \beta - R_{21})}{R_{33}(R_{31} - R_{32} \tan \beta)}, \quad (2.9)$$

where R_{ij} are the elements of the rotation matrix shown in Eq. (2.7). In the same manner as in the R2HDM, the couplings of the neutral scalars to gauge bosons or fermions are given by the respective SM coupling multiplied by a coupling modifier dependent on these angles. For the coupling to electroweak gauge boson pairs, we have

$$g_{h_i V V} = C_i g_{h V V}^{\text{SM}}, \quad (2.10)$$

where [62]

$$C_i = c_\beta R_{i1} + s_\beta R_{i2}. \quad (2.11)$$

The sum rule mentioned in the R2HDM case still applies, with now $C_1^2 + C_2^2 + C_3^2 = 1$. As for the Yukawa Lagrangian, it may be written, for a generic fermion ψ of mass m_f , as

$$\mathcal{L}_Y = - \sum_{i=a,b,c} \frac{m_f}{v} \bar{\psi}_f [c_i^e + i c_i^o \gamma_5] \psi_f h_i, \quad (2.12)$$

with both CP-even fermion interactions – with coupling modifiers c_i^e – and CP-odd ones – with coupling modifiers c_i^o . For model Type I, the coupling modifiers are equal for all fermions, given by [62]

$$c_i^e = \frac{1}{s_\beta} R_{i2}, \quad c_i^o = \frac{1}{t_\beta} R_{i3}. \quad (2.13)$$

For the LS model, the coupling modifiers above apply only to quarks, and to charged leptons one would have

$$c_i^e = \frac{1}{c_\beta} R_{i1}, \quad c_i^o = t_\beta R_{i3}. \quad (2.14)$$

² $\tan \beta$ has the same definition in the real or complex 2HDM, since we have chosen a basis with real vevs for the C2HDM.

For future reference, we will use the following set of input parameters to describe a C2HDM parameter point

$$m_{h_1}, \quad m_{h_2}, \quad m_{H^\pm}, \quad \tan\beta, \quad \text{Re}(m_{12}^2), \quad v = v_{\text{EW}},$$

$$C_2^2, \quad |c(h_2 t \bar{t})|^2, \quad \text{sign}(R_{23}), \quad R_{13}. \quad (2.15)$$

Using this set of input parameters, the third neutral scalar mass m_{h_3} is a dependent parameter and computed according to Eq. (2.9). Note that m_{h_3} can be smaller or larger than m_{h_1} and m_{h_2} , depending on the values of the other parameters shown in Eq. (2.15).

3 Possible indications for a new scalar at 95 GeV

In this section we briefly discuss the current experimental status regarding several excesses observed at a mass of about 95 GeV at LEP and LHC. We will summarize the general properties a scalar state at 95 GeV should have such that it can reproduce those experimental results. For each excess considered below, the signal strengths, or μ values, are defined by the ratio of the observed number of events divided by the expected number of events for a hypothetical SM Higgs boson Φ_{95} with a mass of 95 GeV, *i.e.*,

$$\mu(\Phi_{95})_X = \frac{\sigma(\Phi_{95}) \times \text{BR}(\Phi_{95} \rightarrow X)}{\sigma^{\text{SM}}(\Phi_{95}) \times \text{BR}^{\text{SM}}(\Phi_{95} \rightarrow X)}, \quad (3.16)$$

where $\sigma(\Phi_{95})$ stands for the production cross section of Φ_{95} , and $\text{BR}(\Phi_{95} \rightarrow X)$ is the branching ratio for the decay of Φ_{95} into the final state X .

3.1 The CMS diphoton excess

The LHC searches for diphoton resonances played a vital role for the discovery of the Higgs boson at 125 GeV. Consequently, diphoton searches are also one of the most promising searches for additional Higgs bosons below 125 GeV. The CMS collaboration performed searches for low-mass Higgs bosons decaying into two photons at 8 TeV [63] and 13 TeV [3]. Combining the 8 TeV dataset from Run 1 and the first-year Run 2 data at 13 TeV, corresponding to an integrated luminosity of 19.7 fb⁻¹ and 35.9 fb⁻¹, respectively, CMS observed an excess of 2.8 σ local significance at a mass of 95.3 GeV [3]. This excess can be described by a scalar resonance produced in gluon-fusion production with subsequent decay into diphotons with a signal strength of $\mu(\Phi_{95})_{\gamma\gamma}^{\text{1st-year}} = 0.6 \pm 0.2$. Since this excess was present in both the 8 TeV and 13 TeV data, it has sparked considerable attention in the literature (see, e.g. Refs. [8–14]).

Recently, CMS reported an update of the low-mass Higgs boson searches in the diphoton final state [4]. In this new analysis, the full dataset collected at 13 TeV (but not the Run 1 data collected at 8 TeV) was taken into account, corresponding to an integrated luminosity of 132.2 fb⁻¹. In addition, the updated experimental analysis contains important improvements on the background rejection from misidentified $Z \rightarrow e^+e^-$ Drell-Yan events, and new event classes, demanding additional final state jets, have been used to target different production modes. Notably, CMS observed a local excess with 2.9 σ significance at 95.4 GeV. While the significance of the excess and the preferred mass range are practically unchanged compared to the previous result, the updated analysis is compatible with a scalar resonance with a significantly smaller signal strength of $\mu(\Phi_{95})_{\gamma\gamma} = 0.33_{-0.12}^{+0.19}$ [5] as compared to the value $\mu(\Phi_{95})_{\gamma\gamma}^{\text{1st-year}} = 0.6 \pm 0.2$ reported earlier.

The ATLAS collaboration reported first Run 2 results of searches for scalar resonances decaying into diphotons covering the mass region below 125 GeV using 80 fb^{-1} in 2018 [64]. No excess was observed at masses around 95 GeV. However, the resulting limits were substantially weaker than the corresponding CMS ones, even at 95 GeV where CMS observed the excess. A diphoton resonance consistent with the CMS excess would therefore not have led to a significant excess in this early Run 2 ATLAS search. The final Run 2 results utilizing the full dataset collected at 13 TeV have been reported recently by ATLAS, just three months after CMS reported its full Run 2 results [24]. Therein, the so-called “model-dependent” analysis shows a substantially improved experimental sensitivity compared to the earlier result, which is now at the same level as the CMS analysis. Notably, the most significant excess over the SM expectation observed by ATLAS is at 95.4 GeV, thus in very good agreement with the masses of the excesses observed by CMS. However, the excess is less pronounced, showing a local significance of 1.7σ . Due to the presence of the slight excess, the ATLAS result cannot exclude a possible diphoton signal consistent with the excesses observed by CMS. However, a possible combination of both the ATLAS and the CMS results would give rise to a slightly smaller preferred range of the signal rate of about $\mu(\Phi_{95})_{\gamma\gamma}^{\text{ATLAS+CMS}} \lesssim 0.3$. Since ATLAS did not report a signal strength value corresponding to the observed excess, we will focus in this paper on the description of the excesses observed by CMS based on the publicly reported corresponding signal rate of $\mu(\Phi_{95})_{\gamma\gamma} = 0.33_{-0.12}^{+0.19}$. We note that the conclusions of our results would not change significantly assuming a somewhat smaller diphoton signal rate as suggested by the new ATLAS result. Indeed, a smaller diphoton signal rate at 95 GeV would even allow for a better agreement with flavour physics, as will be seen below.

The fact that the CMS diphoton excess was observed with unchanged significance after the experimental analysis was improved and after the full Run 2 dataset was considered further motivates the investigation of possible interpretations of such a signal in different BSM theories. Even more importantly, however, is the change in the required $\mu(\Phi_{95})_{\gamma\gamma}$ -value. Previously, it was shown that the relatively large value of $\mu(\Phi_{95})_{\gamma\gamma}^{\text{1st-year}} = 0.6 \pm 0.2$ as observed by CMS in the analysis from 2018 could not be described at the level of 1σ in various extensions of the SM. In particular, in the 2HDM constraints from flavour physics in the 2HDM push the mass scale of the BSM scalars to masses with several hundreds of GeV in type II and type IV, such that a state at 95 GeV is incompatible with theoretical constraints (see also Sect. 2). The scalar H in the type I 2HDM has been considered in the past as an origin of the CMS diphoton excess and the LEP excess [9, 10]. However, in order to achieve sufficiently large signal rates of $\mu(H_{95})_{\gamma\gamma}^{\text{1st-year}} \approx 0.6$ the production of H had to be enhanced by additional contributions such as vector-boson fusion production, associated production with a vector boson, or via exotic production modes via decays of $H^\pm \rightarrow HW^\pm$. We note that in this case it is not clear whether the production of H actually describes a signal that is compatible with the excess observed by CMS. In this paper, motivated by the smaller observed signal rate $\mu(\Phi_{95})_{\gamma\gamma} \approx 0.33$ in the updated CMS result, we will revisit the possibility that a BSM state at 95 GeV in the 2HDM is the origin of the diphoton excess. We focus on such cases where this scalar is produced dominantly through gluon-fusion, which is the production channel in which the diphoton excess is most pronounced, without requiring additional production modes. Moreover, we will consider the CP-odd scalar A as an origin of the excess, which is further motivated by another excess observed in ditau final states, see below.

3.2 The CMS ditau excess

Since Higgs bosons are expected to have a coupling to fermions that increases with the fermion mass, it is promising to search for additional Higgs bosons using their decays into third-generation fermions. In the low-mass region below 125 GeV, the decay into top quarks is kinematically forbidden and the decays into bottom quarks are very difficult to search for at the LHC due to the large QCD background. Consequently, the searches for low-mass resonances utilizing ditau final states are particularly important.

Low-mass Higgs-boson searches were performed by CMS including the full Run 2 dataset collected at 13 TeV [6]. Here it was assumed that a scalar resonance is produced via gluon-fusion production and $b\bar{b}$ -associated production, and it subsequently decays into two-lepton pairs, where final states of both leptonically or hadronically decaying tau-leptons were considered. Notably, CMS observed an excess over the background expectation assuming gluon-fusion production at a mass compatible with 95 GeV, without a corresponding excess assuming $b\bar{b}$ -associated production. The excess was found to be most pronounced at a mass hypothesis of 100 GeV, with local and global significances of 3.1σ and 2.7σ , respectively. At a mass of 95 GeV, the local and global significance amount to 2.6σ and 2.3σ , respectively, and the excess can be described by a scalar resonance with a signal strength of $\mu(\Phi_{95})_{\tau\tau} = 1.23^{+0.61}_{-0.49}$ [6]. It should be noted here that the mass resolution in ditau final states is substantially larger compared to the mass resolution of diphoton searches, such that a common origin of both the diphoton and the ditau excesses by means of a scalar resonance at 95 GeV is viable although the ditau excess is most pronounced at a mass of 100 GeV.

So far, no corresponding ATLAS searches for scalar resonances decaying into two tau leptons exist that cover the mass region around 95 GeV.

For a possible BSM interpretation of the ditau excess, we stress that the CMS search specifically targets the gluon-fusion production mode. We think that it is therefore particularly motivated to investigate whether a scalar state of the 2HDM can give rise to a sizable signal in both the CMS ditau and diphoton searches while being dominantly produced via gluon fusion, without relying on additional exotic production modes. In this case, since in the 2HDM the CP-odd state A at 95 GeV has larger gluon-fusion production cross sections than a CP-even state H of the same mass, the investigation of whether the two excesses can be described in terms of the CP-odd Higgs boson A is further motivated. We also note that it has been recently shown in Ref. [21] that a description of the CMS ditau excess by means of a CP-even resonance is in tension with the non-observation of an excess in the CMS searches for $t\bar{t}$ -associated production of a scalar resonance, with subsequent decay into tau-lepton pairs, performed at 13 TeV utilizing the full Run 2 dataset [65]. For a pseudoscalar state, the gluon-fusion production cross section is enhanced due to the different Lorentz structure of the coupling to top quarks, whereas the cross section for $t\bar{t}$ -associated production is smaller as compared to a CP-even state with similar strength of the coupling to top-quarks. In light of this, the description of the ditau excess via a CP-odd state is even more promising.

3.3 The LEP excess strikes back

Previous to the LHC, the LEP e^+e^- collider was in operation at CERN with a maximum center-of-mass energy of 209 GeV until the year 2000. At LEP, searches for the Higgs boson predicted by the SM were performed assuming Higgsstrahlung production with subsequent decay into pairs of bottom-quarks and tau-leptons. These searches excluded a SM Higgs boson up to masses of 114.4 GeV [66]. However, Higgs bosons with masses below 114 GeV are still experimentally

Channel	Signal rate	Local (global) significance
$gg \rightarrow \Phi_{95} \rightarrow \gamma\gamma$	$\mu(\Phi_{95})_{\gamma\gamma} = 0.33_{-0.12}^{+0.19}$ [5]	$2.9(1.3)\sigma$ [4]
$gg \rightarrow \Phi_{95} \rightarrow \tau^+\tau^-$	$\mu(\Phi_{95})_{\tau\tau} = 1.23_{-0.49}^{+0.61}$ [6]	$2.6(2.3)\sigma$ [6]
$e^+e^- \rightarrow Z\Phi_{95} \rightarrow Zb\bar{b}$	$\mu(\Phi_{95})_{bb} = 0.117_{-0.057}^{+0.057}$ [8]	$2.3(< 1)\sigma$ [7]

Table 2: Observed signal rates for a possible new 95 GeV scalar particle.

viable if their couplings to Z bosons are suppressed compared to that of a SM Higgs boson, i.e. $|C_i| < 1$ (see Eq. (2.10)).

The LEP cross section limits extracted from searches for scalar resonances produced in Higgsstrahlung production with subsequent decay into bottom-quark pairs show a mild excess of 2.3σ local significance at a mass of about 98 GeV [67]. The excess is broad due to the hadronic $b\bar{b}$ final state, such that this result is also compatible with a scalar resonance at 95 GeV, consistent with the diphoton and ditau excesses observed by CMS. The excess can be described by a scalar resonance with a signal strength of $\mu(\Phi_{95})_{bb} = 0.117 \pm 0.057$ [8], pointing towards a suppression of the vector boson coupling by roughly an order of magnitude compared to a SM Higgs boson.

An interesting question is therefore whether a scalar state at 95 GeV can describe also this $b\bar{b}$ excess, while at the same time being the origin of the excesses observed by CMS. Since the Higgsstrahlung production mechanism requires a coupling of the scalar to Z bosons, this excess points to an interpretation via a CP-even scalar, whereas an interpretation via a CP-odd state is disfavoured due to the vanishing coupling to vector bosons. As will be discussed in more detail below, the CP-even state H of the 2HDM could give rise to a signal compatible with the LEP excess for values of $|\cos(\beta - \alpha)| \gtrsim \sqrt{0.117} \approx 0.32$. Such departures from the alignment limit are largely excluded by the cross section measurements of the Higgs boson at 125 GeV for all four Yukawa types of the real 2HDM [68, 69]. Even more so for the low- $\tan\beta$ range that we will be focusing on here in order to be able to describe the diphoton excess.

The inclusion of the LEP excess therefore necessitates an extension of the R2HDM. One economic possibility that was considered in Refs. [15, 17, 18, 21, 70, 71] is to extend the 2HDM by an additional real or complex gauge singlet scalar field.³ A dominantly singlet-like scalar state can then be the origin of the diphoton and the LEP excess, where the suppression of the couplings to gauge bosons is achieved via a large singlet admixture of this state.

In this paper we take a different route, and, instead of augmenting the particle content of the 2HDM, we remove the restriction of CP-conservation in the scalar potential. The motivation lies on the fact that scalar states with CP-mixing can potentially be the origin of all three excesses observed at LEP and the LHC.

3.4 Summary of possible signals

In Tab. 2, we summarise the current experimental results regarding the observed excesses in scalar particle searches with a mass close to 95 GeV. In this context “scalar” stands for a spin-0 particle, not its CP quantum numbers – according to the previous discussion we will indeed consider all possible CP properties of this particle (CP-even, CP-odd and CP-mixed).

In our numerical analysis the goal is to predict a Higgs boson at 95 GeV whose signal rates regarding the signatures in which the excesses were observed are in agreement with the measured values shown within one standard deviation, i.e. at the level of 1σ or less (see Tab. 2). At the same time, we ensure that the presence of the state at 95 GeV is not in tension with the other existing cross-section limits from searches in which no deviations have been observed. Note that we will not combine the three channels in a single χ^2 -distribution but instead demand in a more restrictive manner that each excess individually is accommodated within the uncertainty band of ± 1 standard deviation.

3.5 Additional experimental findings regarding a possible state at 95 GeV

We now briefly discuss additional experimental results that can be interpreted as possible hints for a new Higgs boson at 95 GeV but which we do not consider in our analysis since their experimental status is less clear.

For instance, indication for the existence of a Higgs boson at 95 GeV was found in searches for heavy scalar resonances decaying into the discovered Higgs boson at 125 GeV and an another lighter BSM Higgs boson. CMS searched for this cascade decay assuming that the Higgs boson at 125 GeV decays into diphotons and the BSM Higgs boson decays into bottom-quark pairs, giving rise to $\gamma\gamma b\bar{b}$ final states, using the full Run 2 dataset [73]. An excess with local and global 3.8σ and 2.8σ significance was found assuming masses of 650 GeV for the heavy BSM Higgs boson and 90 GeV for the light BSM Higgs boson. However, CMS performed another search with comparable sensitivity for this cascade signature assuming that the Higgs boson at 125 GeV decays into a pair of tau-leptons, giving rise to a $\tau^+\tau^-b\bar{b}$ final states [74]. Therein, no corresponding excess of events over the SM expectation was observed at heavy scalar masses of 600 GeV and 700 GeV (the mass 650 GeV has not been considered). Given the fact that in both analysis the lighter BSM scalar was assumed to decay into bottom-quark pairs, and that due to the broader mass resolution of the $\tau^+\tau^-b\bar{b}$ final state one would expect a slight excess at masses values of 600 GeV and 700 GeV assuming a real signal at 650 GeV consistent with the excess in $\gamma\gamma b\bar{b}$, a model interpretation of the excess in the $\gamma\gamma b\bar{b}$ final state without a corresponding signal in the $\tau^+\tau^-b\bar{b}$ final states appears to be very challenging (see also Ref. [75]). In the 2HDM, a possible interpretation of the excess is in addition disputed by theoretical constraints due to the large mass splitting between 95 GeV and 650 GeV, which can only be accommodated with very large quartic scalar couplings. Consequently, we will not take into account the excess observed in Ref. [73] in our analysis below.

Regarding BSM cascade decays of a heavy resonance decaying into the detected Higgs boson at 125 GeV and another BSM scalar, it is interesting to note that another excess consistent with a scalar resonance at 95 GeV was observed by ATLAS in a search for such signature in

³Interestingly, singlet-extended 2HDMs can additionally accommodate a sizable upwards shift to the prediction of the W -boson mass in the direction of the CDF measurement [72], showing a large disagreement with the SM prediction, via large isospin splittings between neutral and charged scalar states [18]. Moreover, the presence of a complex singlet field allows additionally for the presence of a scalar dark matter candidate at about 62 GeV whose annihilation could be the origin of the galactic-center excess [70].

boosted hadronic final states using novel anomaly detection techniques [76]. This search is based on a fully unsupervised machine learning analysis in order to select possible signal events from the background-only hypothesis, utilizing the full 13 TeV dataset collected during Run 2. The most significant excess for the signature $pp \rightarrow Y \rightarrow X h_{125} \rightarrow q\bar{q}b\bar{b}$, with Y and X being the two BSM scalars, was found for mass intervals of $3608 \text{ GeV} \leq m_Y \leq 3805 \text{ GeV}$ and $75.5 \text{ GeV} \leq m_X \leq 95.5 \text{ GeV}$, where the local and global significances of the excess amount to about 4σ and 1.43σ , respectively, but the excess is, however, not compatible with the expected signal shape. Evidently, as a consequence of the large mass gap between both BSM states this excess cannot be accommodated by means of two states of the same SU(2) scalar doublet without violating perturbativity constraints. Therefore, although the presence of this additional excess hinting at a BSM state at 95 GeV is certainly intriguing, the description of this excess requires extending the 2HDM by additional components, a possibility we do not consider here.

Further claims for an indication of a new resonance at 95 GeV decaying into W -boson pairs have been made in Ref. [77] based on a recasting of CMS [78] and ATLAS [79] searches for $h_{125} \rightarrow W^*W$. However, since the recasting results in indications for a new scalar with a significance above 2σ in a wide mass range from 90 GeV to 180 GeV, the analysis does not point directly to the possible presence of a state at 95 GeV. In addition, in the 2HDM the BSM Higgs bosons have suppressed couplings to gauge bosons, and the decay into W^*W -pairs is highly off-shell for a particle at 95 GeV. An accommodation of a signal in this final state therefore would require very large production cross sections which are, however, excluded based on searches for BSM scalars in other final states. Taking this into account, we do not consider the possibility of an additional signal in W^*W final states in our analysis.

4 2HDM scenarios to reproduce the 95 GeV data

Having reviewed the basic definitions of the model and the possible evidence for signals of a new scalar with mass close to 95 GeV, we will now consider several 2HDM scenarios to fit such signals.

4.1 Parameter scans, theoretical and experimental constraints

In order to investigate whether the 2HDM can describe the observed excesses at 95 GeV, we generated parameter points using the code `ScannerS` [52]. We demand the parameter points to fulfil the following set of theoretical constraints: the potential should be bounded from below (BFB) [29], respect tree-level perturbative unitarity [29] and the electroweak (EW) vacuum should be the global minimum [80, 81].⁴

Additionally, we impose the following experimental constraints: we demand compatibility of the EW precision observables in terms of the oblique parameters S , T and U within a confidence level of 2σ [83], accounting for the experimental correlations between the parameters, and where the theoretical predictions for the oblique corrections were computed at the one-loop level according to Ref. [84]. We fix one of the scalar particles to have the mass of the detected Higgs boson [85], $m_{h_{125}} = 125.09 \text{ GeV}$. We force the mass of other scalars to be outside of a $\pm 5 \text{ GeV}$ mass window around the above value to avoid degenerate states, in which case interference effects would have to be taken into account. Furthermore, we modified the code `ScannerS` to interface

⁴Since a vacuum stability analysis is not the main goal of this paper, we do not consider the physically viable possibility of a long-lived metastable EW vacuum [82], and apply for simplicity the more restrictive condition of an absolutely stable EW vacuum.

with the new package `HiggsTools v.1` [53]. Therein, we use the sub-package `HiggsSignals` [58–60] to check compatibility of the scalar at 125 GeV with the LHC cross section measurements. `HiggsSignals` performs a global χ^2 -fit to a large set of LHC measurements, and based on the χ^2 -value we exclude a 2HDM parameter point if it is disfavoured compared to the SM fit result at more than 2σ confidence level (assuming two-dimensional parameter estimations). For the BSM states, the subpackage `HiggsBounds` [54–57] checks the compatibility of their cross sections with the 95% confidence-level exclusion limits from searches for additional Higgs bosons. `HiggsBounds` selects for each BSM scalar the most sensitive search channel based on the expected cross section limit. For the selected channels the theoretically predicted cross sections are compared against the observed limits, and a point is rejected if for one of the BSM scalars the theory prediction is larger than the experimentally observed limit. Flavour-physics constraints are not yet imposed, but we will include a dedicated discussion of the bounds from flavour physics below, where we consider the compatibility with $B \rightarrow X_s \gamma$ transitions [86–91] in the $m_{H^\pm} - \tan\beta$ plane. In the C2HDM additional constraints from the non-observation of electric dipole moments (EDM) of the electron will be considered separately. Finally, given the focus on this paper, we generate parameter points for which one of the BSM scalars has a mass within the mass window $94 \text{ GeV} \leq m_\phi \leq 97 \text{ GeV}$, where in the R2DHM we have either $\phi = A$ or $\phi = H$, and in the C2HDM $\phi = h_1$ or $\phi = h_2$ depending on whether ϕ is the lightest or the second-lightest neutral scalar, respectively. For both the R2HDM and the C2HDM scenarios, we will give the scanned ranges of the remaining input parameters in the following.

4.2 Real 2HDM type I – $m_A = 95 \text{ GeV}$

In the first scenario we will assume that the possible diphoton signal observed by CMS is produced by the pseudoscalar A , with a mass close to 95 GeV. We fix $m_h = 125.09 \text{ GeV}$, leaving the mass of the other CP-even scalar H and of the charged Higgs to be scanned over. To comply with bounds from searches for charged Higgs bosons at LEP we set $m_{H^\pm} \geq 80 \text{ GeV}$ and consider additionally $m_H \geq 80 \text{ GeV}$. The scanned ranges of the complete set of input parameters are

$$\begin{aligned} m_H &\in [80, 400] \text{ GeV}, & m_A &\in [94, 97] \text{ GeV}, & m_{H^\pm} &\in [80, 400] \text{ GeV}, \\ C_H &\in [-0.3, 0.3], & \tan\beta &\in [1, 3], & m_{12}^2 &\in [10^{-3}, 10^5] \text{ GeV}^2 \end{aligned} \quad (4.17)$$

As discussed, EW precision data constrains the mass splittings of the scalars, which means that it will not be possible to attempt a fit of the diphoton signal within the framework of models Type II or Flipped. In fact, in those models flavour constraints (notably $b \rightarrow s\gamma$ bounds) force the charged mass to be several hundreds of GeV, and hence accommodating $m_A = 95 \text{ GeV}$ is impossible when one combines both S , T and U and unitarity constraints. Therefore, we are left to attempt a fit in models Type I or LS. Let us leave the LS model for later and consider Type I for now.

Identifying the 95 GeV diphoton “signal” with a pseudoscalar means we will not be able to accommodate the LEP $b\bar{b}$ excess – the LEP result involved production of a scalar particle Φ via Higgsstrahlung from a Z boson, which is not possible if Φ is a pseudoscalar. Nevertheless, there are advantages in considering a pseudoscalar when attempting a fit of the LHC diphoton result at 95 GeV: the main production channel is expected to be gluon-gluon fusion and that process yields, for the same mass and similar coupling strengths, larger cross sections for a pseudoscalar than for a CP-even scalar. This is due to the γ_5 matrix in the interactions between quarks and the pseudoscalar, which enhances the quark triangle contribution to the gluon fusion process. Another factor enhancing the cross section in a Type I model relates to the coupling modifiers

for up and down quarks. These have opposite signs (as shown in eq. Eq. (2.4)), which induces a constructive interference between the top and bottom loops contributing to the gluon fusion cross section (this effect had also been observed in [21], see their footnote 2). In fact, using `HiggsTools`, we obtain at N3LO QCD in the heavy-top limit a cross section of about 76 pb for a CP-even SM scalar, i.e. $c_i^e = 1$ and $c_i^o = 0$, with mass of 95 GeV, and about 177 pb for a pseudoscalar of the same mass and couplings $c_i^e = 0$ and $c_i^o = 1$ [92]. With a bottom coupling modifier with the opposite signal to the top one, this number grows to 198 pb. Since all quark couplings of A are multiplied by factors of $\pm 1/\tan\beta$, the cross section for gluon fusion production of the pseudoscalar is therefore simply

$$\sigma(gg \rightarrow A_{95}) = \frac{198}{\tan^2\beta} \text{ pb}. \quad (4.18)$$

In this scenario the phenomenology of the pseudoscalar is quite simple: with a mass of 95 GeV, the decays $A \rightarrow Zh$ and $A \rightarrow ZH$ – which would involve couplings proportional to $\cos(\beta - \alpha)$ and $\sin(\beta - \alpha)$, respectively – are kinematically forbidden, as is $A \rightarrow W^\pm H^\mp$.⁵ Consequently, all possible decays of A involve fermionic couplings (even the decays $A \rightarrow \gamma\gamma$ and $A \rightarrow Z\gamma$), which are all proportional to factors of $|1/\tan\beta|$ in Type I – and hence the branching ratios of A are independent of $\tan\beta$, or indeed of any other scalar potential parameter other than m_A . We find that the branching ratios regarding the channels in which the excesses have been observed are [53, 93]

$$\begin{aligned} \text{BR}(A_{95} \rightarrow \gamma\gamma) &\approx 2.8 \cdot 10^{-4}, \\ \text{BR}(A_{95} \rightarrow b\bar{b}) &\approx 0.72, \\ \text{BR}(A_{95} \rightarrow \tau^+\tau^-) &\approx 0.074. \end{aligned} \quad (4.19)$$

For comparison, the same branching ratios for a CP-even Higgs boson of equal mass are, respectively, $1.4 \cdot 10^{-3}$, 0.81 and 0.082. With these numbers and those mentioned above for cross sections, we obtain

$$\mu(A_{95})_{\gamma\gamma} = \frac{\sigma(gg \rightarrow A_{95}) \text{BR}(A_{95} \rightarrow \gamma\gamma)}{\sigma(gg \rightarrow H_{95}^{\text{SM}}) \text{BR}(H_{95}^{\text{SM}} \rightarrow \gamma\gamma)} \approx \frac{0.52}{\tan^2\beta}. \quad (4.20)$$

Therefore, given that the CMS results (summarised in Tab. 2) indicate that this quantity should vary between 0.21 and 0.52, we obtain the approximate allowed range for $\tan\beta$,

$$1.00 \lesssim \tan\beta \lesssim 1.57. \quad (4.21)$$

For the ditau channel, we will then have

$$\mu(A_{95})_{\tau\tau} = \frac{\sigma(gg \rightarrow A_{95}) \text{BR}(A_{95} \rightarrow \tau\tau)}{\sigma(gg \rightarrow H_{95}^{\text{SM}}) \text{BR}(H_{95}^{\text{SM}} \rightarrow \tau\tau)} \approx \frac{2.35}{\tan^2\beta}, \quad (4.22)$$

which, according to table 2, gives a preferred $\tan\beta$ range of

$$1.13 \lesssim \tan\beta \lesssim 1.78. \quad (4.23)$$

Thus, we see that the range of $\tan\beta$ necessary to fit the diphoton signal at 95 GeV intersects with the one required to fit the ditau signal.

⁵Even if the final state particles in these decays are off-shell, we can expect them to be highly suppressed.

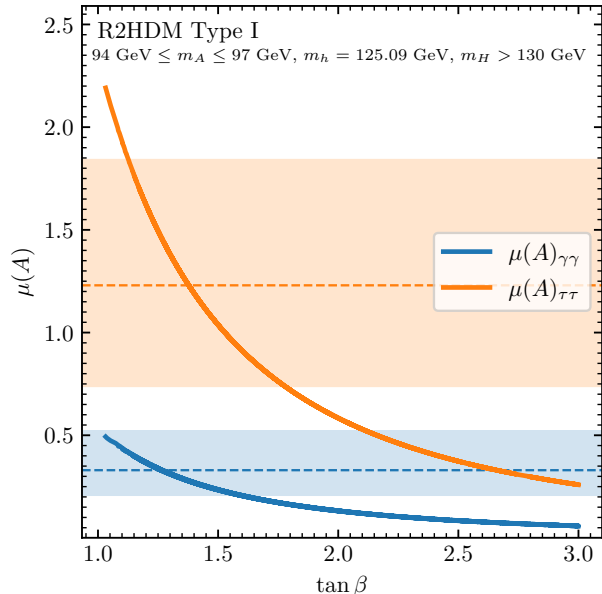


Figure 1: Signal rates for the diphoton and ditau excesses *vs* $\tan\beta$ for a 95 GeV pseudoscalar within the Type I 2HDM. Except for constraints from flavour physics, all theoretical and experimental constraints are applied. The bands correspond to the experimentally observed signal rates within their 1σ uncertainty band (see Tab. 2).

This is shown in Fig. 1, where we present the results of a scan over the real 2HDM parameter space. Notice that flavour bounds were not (yet) imposed but all other constraints (electroweak precision constraints; unitarity; boundedness from below; Higgs precision data and new scalar search bounds) have been implemented via `ScannerS` and `HiggsTools`. From all those cuts, we find that $m_H \in [85, 370]$ GeV, $m_{H^\pm} \in [150, 370]$ GeV, and will be discussed in detail in Sect. 4.2.2. The crucial observation to be made from Fig. 1 is that both signal rates can be fitted in the range of $\tan\beta$ discussed above. Now, if we consider a possible combination with ATLAS, then the preferred region of the diphoton signal rate would be constrained to somewhat smaller values. This would reduce slightly the upper end of the blue bar, but as seen in Fig. 1 this would not alter the general statement that both rates can be fitted simultaneously.

We can further characterize the region where both $\mu(A_{95})_{\gamma\gamma}$ and $\mu(A_{95})_{\tau\tau}$ are fitted. The requirement that the scalar h be SM-like pushes us to the alignment limit, with $|\cos(\beta - \alpha)|^2 \lesssim 0.1$, see discussion in Sect. 4.2.1. Another interesting observation concerns the soft breaking parameter m_{12}^2 – with the low masses found for all extra scalars, this parameter is not necessary in these scenarios. Recall that m_{12}^2 is introduced to allow for a decoupling limit, where the non-SM-like scalars can be indefinitely large. That is not the situation in this case, where a scalar at 95 GeV is set to fit the diphoton and/or diphoton excesses. Indeed, a dedicated scan with $m_{12}^2 = 0$ confirmed that the conclusions reached here hold true. The possibility of fitting both excesses in the framework of a Type-I 2HDM with an unbroken \mathbb{Z}_2 is quite interesting, since in that model the number of free parameters in the scalar sector (7) is exactly equal to the number of parameters which can be determined directly from experimental measurements.⁶

⁶These parameters would be the EW vev v (determined from the gauge boson masses and the Fermi constant), $\tan\beta$ (determined, e.g. from the signal rates of A_{95}), $\sin(\beta - \alpha)$ (determined from the coupling measurements of h) and the four masses, m_h , m_H , m_A and m_{H^\pm} . If $m_{12}^2 \neq 0$, the determination of the model parameters would be more involved.

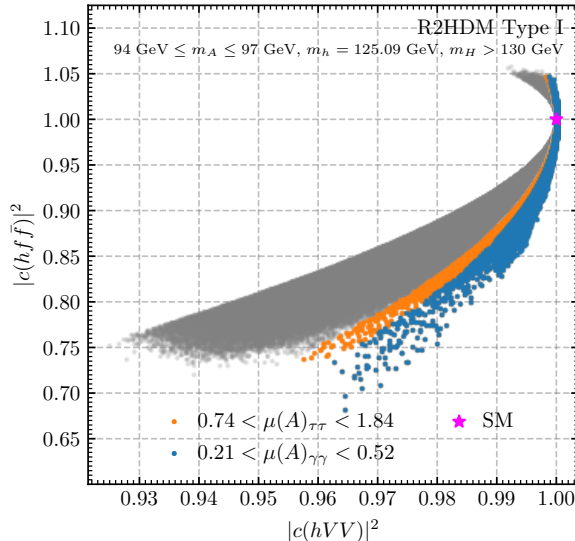


Figure 2: Squared coupling coefficient of $h = h_{125}$ to gauge bosons $|c(h_{125}VV)|^2$ vs. to fermions $|c(h_{125}f\bar{f})|^2$. The blue and orange points predict a signal rate for the diphoton and the ditau excess within the experimentally observed 1σ uncertainty bands, respectively (see Tab. 2). Blue points are plotted on top of orange points. The remaining points are shown in grey. The SM prediction for the couplings coefficients is indicated with a magenta star.

4.2.1 Properties of $h = h_{125}$

As already discussed in Sect. 1 and Sect. 3, a wide class of models had been proposed in the literature already for a description of the diphoton excess at 95 GeV. In many cases [8, 11, 13], these models incorporate a gauge-singlet scalar state at 95 GeV which acquires its couplings to the fermions and gauge bosons by means of a mixing with the detected Higgs boson at 125 GeV. These constructions, therefore, predict modifications of the couplings of the detected Higgs boson compared to the SM predictions. In the R2HDM interpretation presented here, with the CP-odd state being the origin of the diphoton and the ditau excess, no mixing between A_{95} and the detected Higgs boson h is required for a description of the excesses. Consequently, the R2HDM interpretation of the diphoton excess and the ditau excess is possible without the presence of a modification of the couplings of the detected Higgs boson at 125 GeV with respect to the SM.

This is seen in Fig. 2, in which we show the squared coupling coefficients of h , also denoted κ -factors in the literature, to gauge bosons on the horizontal axis and for the to fermions on the vertical axis, respectively. The SM prediction $\kappa_V^2 = \kappa_f^2 = 1$ is indicated with the magenta star. One can see that we find points describing the diphoton excess (blue points) and the ditau excess (orange points) in the whole allowed range of κ_f^2 . In particular, blue and orange points are found in and around the alignment limit, in which the state h is effectively indistinguishable from a SM Higgs boson. The allowed intervals of the κ -factors in Fig. 2 are constrained by the LHC cross section measurements of the detected Higgs boson. One can see that there is more freedom from departures of the alignment limit for $\kappa_f < 1$ compared to the case with $\kappa_f > 1$. The origin of this asymmetry are several LHC measurements showing slight deviations from the SM, giving rise to a preference for a small preference for $\kappa_f^2 < \kappa_V^2$, (see Ref. [68] for a more detailed discussion). This observation is independent of the specific R2HDM scenario under investigation here and, accordingly, not correlated with the predictions regarding the signal rates of the pseudoscalar, A_{95} .

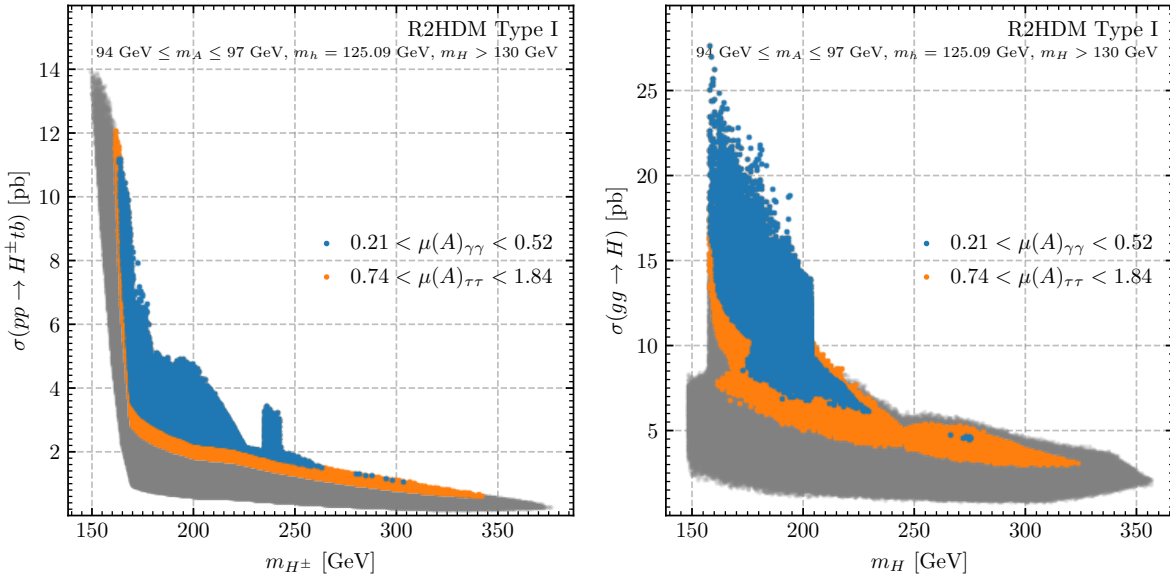


Figure 3: The cross sections $\sigma(pp \rightarrow H^\pm tb)$ vs m_{H^\pm} (left) and $\sigma(gg \rightarrow H)$ vs m_H (right) for the scanned points within the Type I 2HDM. Except for flavour physics, all theoretical and experimental constraints are applied. The blue and orange points predict a signal rate for the diphoton and the ditau excess within the experimentally observed 1σ uncertainty bands, respectively (see Tab. 2). Blue points are plotted on top of orange points. The remaining points are shown in grey.

4.2.2 Properties of the other BSM states

More interesting are the results shown in Fig. 3, where we show the predicted values for the dominant LHC production cross sections of H^\pm (left) and H (right) against their masses. Due to the low values of $\tan\beta$ considered here, H^\pm is mainly produced in association with a top and a bottom quark, and H is mainly produced via gluon-fusion production. We show the points that predict values for $\mu(A_{95})_{\gamma\gamma}$ and $\mu(A_{95})_{\tau\tau}$ in agreement with the observed values in blue and orange, respectively, while the remaining points are shown in grey. As before, all theoretical and experimental constraints are applied, barring flavour. We observe a clear predilection for masses of both H^\pm and H lower than roughly 250 GeV, where the diphoton excess is accommodated with cross sections between 2 pb and 14 pb for the charged scalar, and 5 pb and 25 pb for the heavier CP-even state H . The ditau excess by itself allows a wider range of masses and cross sections, reflecting the fact that a description of this excess is compatible with larger values of $\tan\beta$ compared to the diphoton excess (see Eq. (4.23) and Eq. (4.21)).

Using `HiggsBounds`, we find that the presence of H^\pm in this scenario is mainly constrained via searches for $pp \rightarrow H^\pm tb$ with subsequent decay of $H^\pm \rightarrow tb$, which were performed by the ATLAS collaboration including the full Run 2 dataset [94] and by the CMS collaboration using 35.9 fb^{-1} collected at 13 TeV [95], all of which covering a mass range above 200 GeV.⁷ The blue points, which fit the CMS diphoton excess, are limited to a relatively small region in the mass interval of $165 \text{ GeV} \lesssim m_{H^\pm} \lesssim 250 \text{ GeV}$. This region is so far compatible with the cross section limits from searches for $H^\pm \rightarrow tb$ but will be within the reach of LHC as the luminosity increases. This provides a clear target to further probe the R2HDM interpretation of the CMS diphoton excess at 95 GeV in the future. We finally note that the sharp increase of the predicted cross sections of H^\pm at masses below about 165 GeV results from the additional production of H^\pm via

⁷Depending on the experimental resolution, the limits are applied also for masses slightly below 200 GeV.

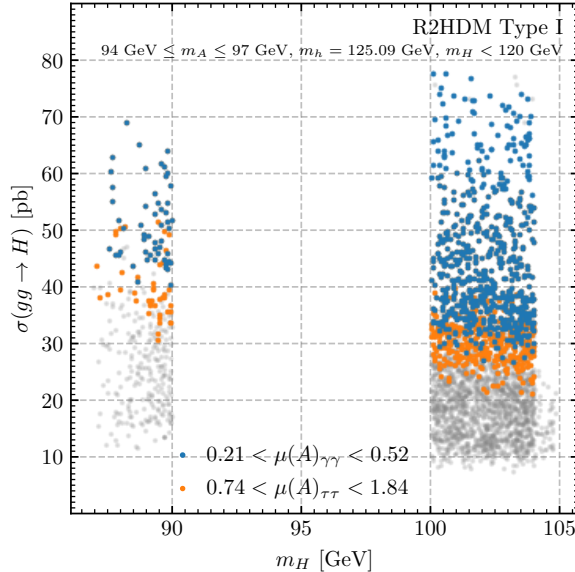


Figure 4: Same as Fig. 3 but showing all scan points with $m_H < 120$ GeV. The mass window $90 \text{ GeV} < m_H < 100 \text{ GeV}$ was excluded in our analysis to avoid degenerate neutral scalar states, see discussion in the text.

$pp \rightarrow t\bar{t}$ production with the top-quark decaying to H^\pm and a bottom quark, (see Ref. [96] for details). This increase of the cross sections gives rise to a lower limit of $m_{H^\pm} \gtrsim 150 \text{ GeV}$ due to the limits from searches for H^\pm decaying into a tau-lepton and a neutrino [97] and due to the measurements of the branching ratios of ordinary top-quark decays. In summary, only a small mass window around 200 GeV remains allowed for H^\pm , where it is too heavy to be produced in large numbers via (off-shell) top-quark decays, but also light enough to escape the LHC searches for $H^\pm \rightarrow tb$.

Turning now to the second CP-even Higgs boson H , one can see in the right plot of Fig. 3 that parameter points describing the CMS diphoton excess (blue points) can be found only in a narrow mass interval of $170 \text{ GeV} \lesssim m_H \lesssim 225 \text{ GeV}$. Within this interval, the CMS searches for H decaying into a pair of Z -bosons including 35.9 fb^{-1} collected at 13 TeV [98] give rise to the upper limits on the gluon-fusion production cross sections of H . For masses of $m_H \gtrsim 200 \text{ GeV}$, we observe a sharp decrease of the allowed values of the cross sections, almost excluding the possibility of a description of the diphoton excess. This decrease of the maximal allowed values of $\sigma(gg \rightarrow H)$ result from searches for the cascade decay $H \rightarrow ZA$, where here $A = A_{95}$ is the state responsible for the description of the excesses at 95 GeV (see also Ref. [20]), which have been performed by the CMS collaboration at 8 TeV assuming that A decays into a pair of bottom quarks or a pair of tau leptons [99], and at 13 TeV assuming $A \rightarrow b\bar{b}$ [100]. We note that the corresponding ATLAS analysis, including already the full Run 2 data set, does not cover the mass region below 125 GeV for the state A , and is therefore not applicable here. The lower limit on m_H , for which blue (and orange) points are found, is determined by the CMS cross section limits from searches for scalar resonances decaying into tau lepton pairs, which have been performed at 13 TeV using the full Run 2 data set [6]. This search becomes the most sensitive channel for the presence of H at masses below the kinematic threshold for the decays $H \rightarrow VV$, where the branching ratios for $H \rightarrow \tau^+\tau^-$ become sizable. Again, we note that the corresponding ATLAS search for scalar resonance decaying into tau-lepton pairs is not applicable here because light masses below 200 GeV are not covered in the analysis [101].

As noted, we also find parameter points where there is a second CP-even scalar with a mass below 125 GeV. We focus on the case where we force non-degeneracy of masses between the scalars. We show the corresponding results in Fig. 4, where one can observe that the cross section can grow up to values of about 80 pb for masses of H slightly above 100 GeV. The most sensitive search channels for most parameter points are LHC searches for the decay $H \rightarrow \tau^+ \tau^-$ at 13 TeV, which were published in Ref. [6, 102] assuming that H is produced via gluon-fusion, and in Ref. [65] assuming the production of H in association with top-quark pairs. The masses of the charged Higgs bosons in this scenario are found in the range $140 \text{ GeV} \lesssim m_{H^\pm} \lesssim 175 \text{ GeV}$, where the phenomenology is unchanged compared to the case with $m_H > 130 \text{ GeV}$ as discussed in Sect. 4.2.2.

Interestingly, the parameter points with $m_H \approx 100 \text{ GeV}$ open up a further possibility to describe the excesses observed by CMS. We find that in this case the cross sections for the process $gg \rightarrow H \rightarrow \tau^+ \tau^-$ can be large enough to accommodate the ditau excess (which actually was most pronounced at 100 GeV), while the diphoton excess is accommodated by means of the pseudoscalar state A . In order to accurately determine whether the ditau excess is described in agreement with the experimental observations, one would have to study the impact of both the contributions of A and H to the possible ditau signal, and verify whether the observed excess is sufficiently broad that one can sum both contributions (where interference effects do not play a role if CP-conservation is imposed), or whether both states would be observed as two distinguishable signals in the ditau invariant-mass spectrum. Since we focus here on the possibility to accommodate the collider excesses by means of a single BSM particle, which we regard as a theoretically more economical description providing more specific predictions to probe the scenarios in the future, we do not study in detail the case with two particles contributing to the possible ditau signal.

4.2.3 Flavour-physics constraints

Finally, let us consider the impact of flavour constraints in these results. For a Type I model, the strongest bounds on the 2HDM parameter space – usually expressed as excluded areas in the $\tan\beta$ - m_{H^\pm} plane – come from $b \rightarrow s\gamma$ measurements [33]. Almost as restrictive are the bounds from Δm_{B_s} , the mass difference between the B_s and \bar{B}_s neutral mesons. In Fig. 5, we display the totality of our scan in the $\tan\beta$ - m_{H^\pm} plane, where the regions below the black dotted and dashed lines are excluded at 2σ and 3σ confidence level, respectively. These lines were obtained using `SuperIso` [103, 104] for the theoretical predictions for $\text{BR}(b \rightarrow s\gamma)$, and comparing them to the experimentally measured central value and ± 1 standard deviations shown in Eq. (4.25). Blue points predict a value of $\mu(A_{95})_{\gamma\gamma}$ within the 1σ uncertainty interval. In the same manner, orange points predict a value of $\mu(A_{95})_{\tau\tau}$ compatible with the measured value within 1σ . We recognise that the blue points, providing a good description of the diphoton excess, are disfavoured by the flavour constraints at a confidence level of about 2.5σ or more. We note that this tension would be weaker to some degree assuming a combined ATLAS+CMS diphoton signal rate, which would be compatible with slightly larger $\tan\beta$ values.

In order to further quantify this, let us recall that there are considerable uncertainties in the calculation of the $b \rightarrow s\gamma$ branching ratio already at the SM, stemming from choices of renormalization or fragmentation scales. The SM prediction for this branching ratio (see [91]) gives

$$\text{BR}(b \rightarrow s\gamma)_{E_\gamma > E_0 = 1.6 \text{ GeV}} = (3.40 \pm 0.17) \times 10^{-4}, \quad (4.24)$$

and the experimentally measured value for this quantity from the HFLAV Collaboration [105]

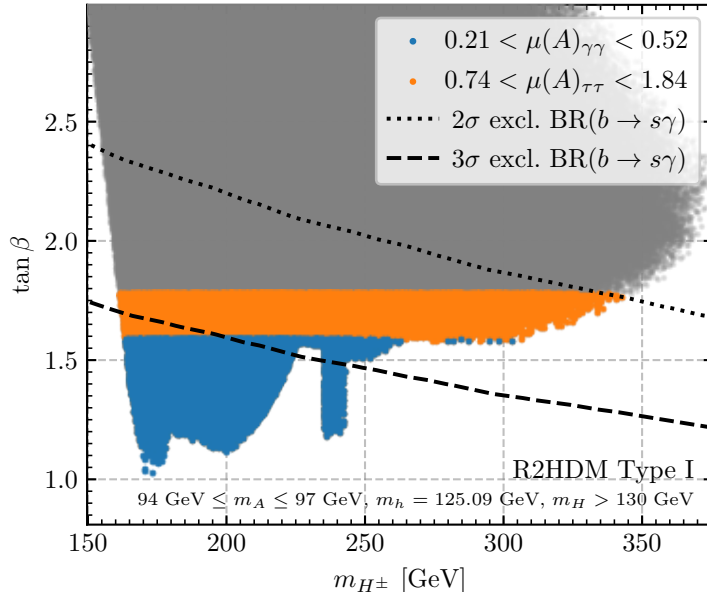


Figure 5: Flavour constraints in the m_{H^\pm} – $\tan\beta$ plane. The regions below the black dotted and dashed lines are excluded at 2σ and 3σ confidence level, respectively. Grey points are the totality of our scan; orange points are restricted to $0.74 < \mu(A)_{\tau\tau} < 1.84$; and blue points are further restricted to $0.21 < \mu(A)_{\gamma\gamma} < 0.52$.

is

$$\text{BR}(b \rightarrow s\gamma)_{E_\gamma > E_0 = 1.6 \text{ GeV}} = (3.49 \pm 0.19) \times 10^{-4}. \quad (4.25)$$

In the 2HDM, the $b \rightarrow s\gamma$ branching ratio includes the SM value plus a deviation δ containing charged Higgs contributions [34],

$$\text{BR}(b \rightarrow s\gamma)_{E_\gamma > E_0} = \text{BR}(b \rightarrow s\gamma)^{\text{SM}} + \delta\text{BR}(b \rightarrow s\gamma), \quad (4.26)$$

so that the quantity $\delta\text{BR}(b \rightarrow s\gamma)$ must be smaller than some combination of the theoretical and experimental errors above. If one takes $|\delta\text{BR}(b \rightarrow s\gamma)| < 2.5 \times 10^{-5}$, this reproduces with very good approximation the exclusion region from [33]. Using the NLO expressions from [34]⁸, we find that the blue or orange points from Fig. 5 yield $|\delta\text{BR}(b \rightarrow s\gamma)| \simeq (4 - 14) \times 10^{-5}$. Therefore, unless a non-2HDM contribution to the flavour sector is introduced to account for this divergence, the interpretation of the diphoton excesses at 95 GeV as a Type-I pseudoscalar A is in tension with the current experimental $b \rightarrow s\gamma$ results. It should be added that it is possible to satisfy the $b \rightarrow s\gamma$ bound in a larger mass regime: with m_H and m_{H^\pm} above about 500 GeV, it is possible to accommodate the values of $\tan\beta$ required to fit both $\mu(A_{95})_{\gamma\gamma}$ and $\mu(A_{95})_{\tau\tau}$. However, in that regime there are strong constraints from searches in the $H \rightarrow ZA \rightarrow ll\bar{b}\bar{b}$ channel [100] – notice that the vertex HZA is proportional to $\sin(\beta - \alpha) \simeq 1$ – so the decay $H \rightarrow ZA$ is not at all suppressed despite proximity to the alignment limit. And with H masses above 500 GeV and $m_A = 95$ GeV, phase-space suppression does not affect this decay either. Moreover, masses of $250 \text{ GeV} \lesssim m_{H^\pm} \lesssim 350 \text{ GeV}$ with $\tan\beta < 2$ (as favoured by the excesses) are excluded by LHC searches for $H^\pm \rightarrow tb$ (see Fig. 3) and even larger values of m_{H^\pm} are in tension with theoretical constraint from perturbative unitarity due to the large mass splitting between A_{95} and H^\pm .

⁸NLO contributions account for a 15% to 20% correction on the LO result.

4.3 Real 2HDM type I – $m_H = 95$ GeV

Another obvious possibility within the R2HDM would be to attempt to explain the CMS di-photon excess as being produced by the CP-even scalar H . This would also raise the possibility of a simultaneous explanation of the LEP excess, since H could have been produced via Higgsstrahlung at LEP. However, a dedicated scan of this possibility – fixing $m_H \simeq 95$ GeV and allowing $m_A, m_{H^\pm} > 130$ GeV to vary freely – leads to no satisfactory conclusions. To wit, the only way of having values of $\mu(H)_{\gamma\gamma}$ above 0.21 would be to have $\tan\beta \lesssim 0.6$, and this could only be achieved in the LS model. In that case the CMS di-tau excess could be accommodated for $\tan\beta \geq 1$, incompatible with the $\tan\beta$ -values required for a description of the diphoton excess. In a Type I model the results are even worse, with maximum values of $\mu(H)_{\gamma\gamma}$ of the order of 0.03 obtained for $\tan\beta \simeq 1.5$, and $\mu(H)_{\tau\tau}$ smaller than 0.6 for all scan points. In both cases, no possibility of reproducing the LEP excess was found due to the constraints on the signal rates of the Higgs boson at 125 GeV, setting tight upper limits on the strength of the coupling of H to Z bosons due to the sum rule discussed below Eq. (2.2). Taking all these limitations into account, we do not discuss the scenarios with $m_H \simeq 95$ GeV any further.

4.4 Real 2HDM type LS

Besides a Type I Yukawa model, the lepton specific (LS) 2HDM also allows for light scalar spectra with masses around 125 GeV without strong disagreements with flavour-physics constraints, measurements of EWPO, or theoretical requirements of perturbativity. Here, we briefly comment on the possibility of describing the excesses at 95 GeV in the LS R2HDM. We can obtain a semi-analytical understanding of the predictions of the LS model for $\mu(A_{95})$. Since only the leptonic coupling modifier changes compared to Type I, the expression of the cross section on $\tan\beta$ shown in Eq. (4.18) is the same for both models. From Eq. (4.19), we also see that $BR(A \rightarrow \tau\tau)$ is already small compared to other decay channels. The branching ratios for A in the LS model now have a non-trivial $\tan\beta$ dependence – the leptonic decay widths are proportional to $\tan^2\beta$ – all others proportional to $1/\tan^2\beta$ ⁹. With Γ_A being the total width of the pseudoscalar A , we can use the numbers of Eq. (4.19) and single out expressions for several widths with their explicit $\tan\beta$ dependences,

$$\begin{aligned}\Gamma(A \rightarrow \gamma\gamma) &\simeq \frac{2.8 \times 10^{-4}}{\tan^2\beta} \Gamma_A, \\ \Gamma(A \rightarrow \tau\tau) &= 0.074 \tan^2\beta \Gamma_A, \\ \Gamma(A \rightarrow \text{Not } \tau's) &\simeq \frac{1 - 0.074}{\tan^2\beta} \Gamma_A.\end{aligned}\tag{4.27}$$

With these approximate expressions, we can write

$$BR(A \rightarrow \gamma\gamma) = \frac{\Gamma(A \rightarrow \gamma\gamma)}{\Gamma(A \rightarrow \text{Not } \tau's) + \Gamma(A \rightarrow \tau\tau)} \simeq \frac{2.8 \times 10^{-4}}{0.926 + 0.074 \tan^4\beta}\tag{4.28}$$

and likewise we obtain

$$BR(A \rightarrow \tau\tau) = \frac{\Gamma(A \rightarrow \tau\tau)}{\Gamma(A \rightarrow \text{Not } \tau's) + \Gamma(A \rightarrow \tau\tau)} \simeq \frac{0.074}{0.926 + 0.074 \tan^4\beta} \tan^4\beta.\tag{4.29}$$

⁹Neglecting the leptonic contributions to $A \rightarrow \gamma\gamma$, which is a good first approximation.

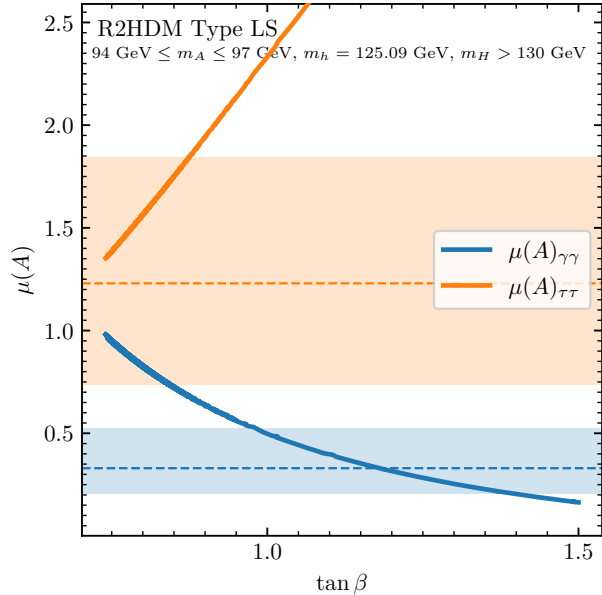


Figure 6: Signal rates for the diphoton and ditau excesses *vs* $\tan\beta$ for a 95 GeV pseudoscalar within the Lepton Specific 2HDM. Except for constraints from flavour physics, all theoretical and experimental constraints are applied. The bands correspond to the experimentally observed signal rates within their 1σ uncertainty band (see Tab. 2).

We therefore see that both branching ratios have very different $\tan\beta$ dependences, which leads us to (using the cross section from Eq. (4.18))

$$\begin{aligned}\mu(A_{95})_{\gamma\gamma} &= \frac{0.52}{(0.926 + 0.074 \tan^4 \beta) \tan^2 \beta} \\ \mu(A_{95})_{\tau\tau} &= \frac{2.35 \tan^2 \beta}{0.926 + 0.074 \tan^4 \beta}\end{aligned}\quad (4.30)$$

which reproduce quite accurately the results of our scan, shown in Fig. 6. As we see from this plot, there is no region of $\tan\beta$ values for which both diphoton and ditau signals can be fitted simultaneously. The ditau signal can be fitted, but only for values of $\tan\beta$ below 1, and the diphoton signal once again requires $1.0 \lesssim \tan\beta \lesssim 1.3$. In both cases, as in the Type I 2HDM, such small $\tan\beta$ -values are in significant tension with constraints from flavour physics. Since the LS Yukawa type does not allow for a description of the diphoton excess, which is the main motivation for this paper, as discussed above, we will not consider the LS type in the following discussion.

4.5 Complex 2HDM – $m_{h_1} = 95$ GeV, $m_{h_2} = 125$ GeV, $m_{h_3} > 130$ GeV

As we have seen in the previous section, it is possible to describe well the 95 GeV diphoton and ditau excesses via a pseudoscalar within the CP-conserving Type-I 2HDM but the corresponding parameter space was found to be in tension with flavour-physics constraints, namely the $b \rightarrow s\gamma$ bounds. Furthermore, a pseudoscalar cannot serve as an origin for the LEP $b\bar{b}$ excess. A CP-even scalar with mass equal to 95 GeV cannot describe the diphoton excess in this model without even more strenuous violations of flavour bounds due to the low values for $\tan\beta$ required. It is, therefore, of interest to attempt a description of the excesses within the wider framework of the

C2HDM. In this model, all scalars have in general mixed CP-properties and one can envision a 95 GeV particle with a significant CP-odd component, by means of which the particle can account for the LHC diphoton and ditau excesses, and a CP-even component large enough to produce the possible $b\bar{b}$ signal at LEP.

Other possible advantages arising from the C2HDM are: (a) a widening of the available parameter space, due to an extra parameter in the model; (b) greater flexibility in complying with Higgs precision data, since the gluon-gluon production cross section now includes contributions from both CP-even and CP-odd channels; (c) possible larger values for the branching ratios for the diphoton decay of the 95 GeV particle than would be obtained for a pure pseudoscalar.¹⁰

We, therefore, undertook a parameter scan of the C2HDM, following the procedures outlined in Sect. 2, including all theoretical (boundedness from below; unitarity; vacuum stability) and experimental constraints (electroweak precision bounds; Higgs precision data; extra scalar searches), with the exception of flavour physics and electron dipole moment (EDM) measurements. In the C2HDM, the latter may become relevant [106], and we will address both separately in the following discussion. The scanned ranges of the complete set of input parameters of the C2HDM are

$$\begin{aligned} m_{h_1} &\in [94, 97] \text{ GeV}, & m_{h_2} &= 125.09 \text{ GeV}, & m_{H^\pm} &\in [80, 400] \text{ GeV}, \\ \text{Re}(m_{12}^2) &\in [10^{-3}, 10^5] \text{ GeV}^2, & C_2^2 &\in [0.75, 1], & |c(h_2 u \bar{u})|^2 &\in [0.8, 1.2], & \tan \beta &\in [1, 3], \\ R_{13} &\in [-1, 1], & \text{Sign}(R_{23}) &\in [-1, 1] \end{aligned} \quad (4.31)$$

According to Eq. (2.9), specifying two of the neutral masses, $\tan \beta$ and the mixing matrix R , the third mass m_{h_3} is fixed by the parameters shown in Eq. (4.31). There are then three possibilities, (i) $m_{h_3} > 125$ GeV, (ii) $95 < m_{h_3} < 125$ GeV and (iii) $m_{h_3} < 95$ GeV. Option (i) seems the most natural way to accommodate a scalar with 95 GeV, since options (ii) and (iii) would imply the existence of two lighter scalars than the SM-like state with mass 125 GeV discovered at the LHC.¹¹ We will therefore deal with option (i) for this section, and briefly address the other two in Sect. 4.6.

The results of our C2HDM scan in the mass hierarchy with $m_{h_1} \approx 95$ GeV, $m_{h_2} = 125.1$ GeV and $m_{h_3} > 130$ GeV (we only consider non-degenerate scenarios, see Sect 4.1) are shown in Fig. 7, where we plot, as a function of $\tan \beta$, the values of the signal rates $\mu(h_1)_{\gamma\gamma}$, $\mu(h_1)_{\tau\tau}$ and $\mu(h_1)_{bb}$ (the latter concerning LEP results, the former two LHC ones) in blue, orange and green, respectively. We see that the diphoton excess can be reproduced for $1.0 \lesssim \tan \beta \lesssim 2.5$, a wider interval than the one found for the real 2HDM (see Fig. 1). A joint fit with the ditau signal reduces the upper bound on $\tan \beta$ to roughly 1.8. As for the LEP excess, we see that the lower values of the 1σ interval for this signal are reproduced in the C2HDM more or less independently of $\tan \beta$ (at least for the restricted scan we undertook here). Remarkably, we see that for $1.0 \lesssim \tan \beta \lesssim 1.8$ all three possible 95 GeV signals may be described individually in the C2HDM. Even more strikingly, the parameter points with $\tan \beta \lesssim 1.5$ predict signal rates regarding all three excesses within the respective experimentally observed 1σ uncertainty bands, indicating that the excesses can be fitted simultaneously in the C2HDM, in contrast to the observation in the R2HDM in which no sizable signal at LEP was present. Again, a possible combination of the di-photon search results of both CMS and ATLAS does not alter the general

¹⁰In fact, for a CP-odd state of mass 95 GeV ($c_i^e = 0$ and $c_i^o = 1$) the branching ratio for the diphoton decay is 2.8×10^{-4} , whereas for a CP-even SM-like state ($c_i^e = 1$, $c_i^o = 0$) of the same mass one finds 1.4×10^{-3} .

¹¹And paraphrasing Wilde, to lose one scalar may be regarded as a misfortune; to lose both looks like carelessness.

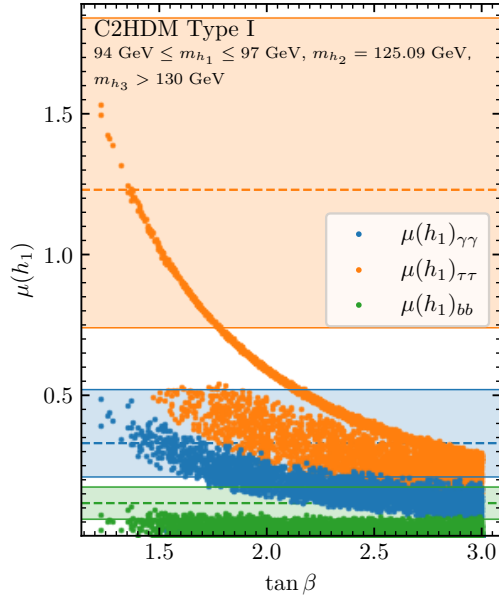


Figure 7: Signal rates for the diphoton (blue), ditau (orange) and $b\bar{b}$ (green) excesses *vs* $\tan\beta$ for a 95 GeV scalar within the Type I C2HDM and $m_{h_3} > 130$ GeV. Except for constraints from flavour physics and EDMs, all theoretical and experimental constraints are applied. The bands correspond to the experimentally observed signal rates within their 1σ uncertainty band (see Tab. 2).

statement. If the diphoton signal rate would be constrained to slightly smaller values, as the ATLAS result suggests, the three excesses could still be fitted simultaneously.

In Fig. 8, we show how the several excesses are correlated in order to shed more light on the possibility of describing the three excesses together. An increase in $\mu(h_1)_{\gamma\gamma}$ implies an increase in $\mu(h_1)_{\tau\tau}$, with predilection for lower values of $\mu(h_1)_{bb}$. Fitting the LEP excess is relatively easy in this version of the C2HDM, due to the larger allowed values for the coupling between h_1 and Z bosons compared to the real 2HDM case. Indeed, for the real 2HDM, as seen in the previous section, the coupling modifier between a CP-even 95 GeV scalar and electroweak gauge bosons was found to be $|C_H| = |\cos(\beta - \alpha)| \lesssim 0.2$ for the parameter points that provide a good description of the diphoton excess. In contrast, for the C2HDM scan with the mass hierarchy studied in this section, we find also values of $|C_1| \approx 0.3$ (see Eq. (2.11)).

4.5.1 Properties of $h_2 = h_{125}$

Compared to the R2HDM scenario discussed in Sect. 4.2, the C2HDM scenario presented here has the additional goal of accommodating the excess observed at LEP, for which the state at 95 GeV has to be produced in Higgsstrahlung. Hence, in this case, departures from the alignment limit of the 2HDM are required, since otherwise only the scalar playing the role of the SM-like Higgs boson at 125 GeV would couple to gauge bosons, while the other neutral scalars would not couple to Z bosons and accordingly would not be produced. Moreover, if CP-violation is taken into account, all neutral scalar states can potentially mix with each other. In contrast, in the CP-conserving R2HDM there is a purely CP-odd scalar state and only the two CP-even scalar states can mix among each other. Given these additional sources of modifications of the couplings of $h_2 = h_{125}$, it is even more interesting to scrutinize the predictions for the couplings of h_{125} and the possibility of using the detected Higgs boson at 125 GeV as a probe of the

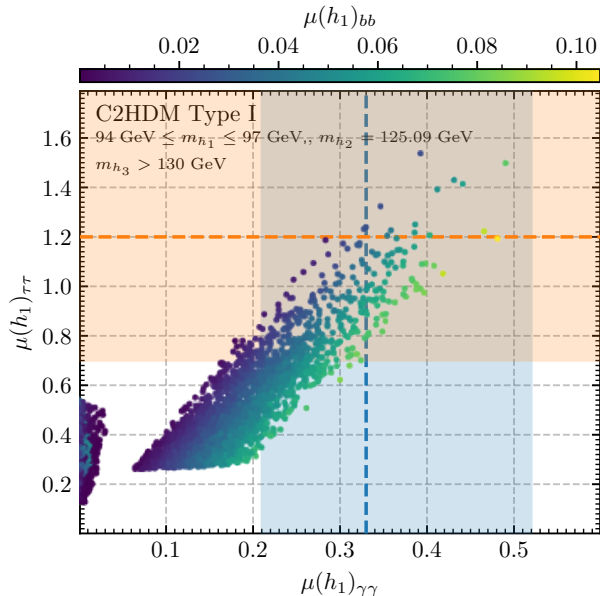


Figure 8: Diphoton signal rate $\mu(h_1)_{\gamma\gamma}$ vs ditau signal rate $\mu(h_1)_{\tau\tau}$ for a 95 GeV scalar within the Type I C2HDM. Except for constraints from flavour physics and EDMs, all theoretical and experimental constraints are applied. The colour coding of the points indicates the values of $\mu(h_1)_{bb}$. The bands correspond to the experimentally observed signal rates within their 1σ uncertainty band (see Tab. 2).

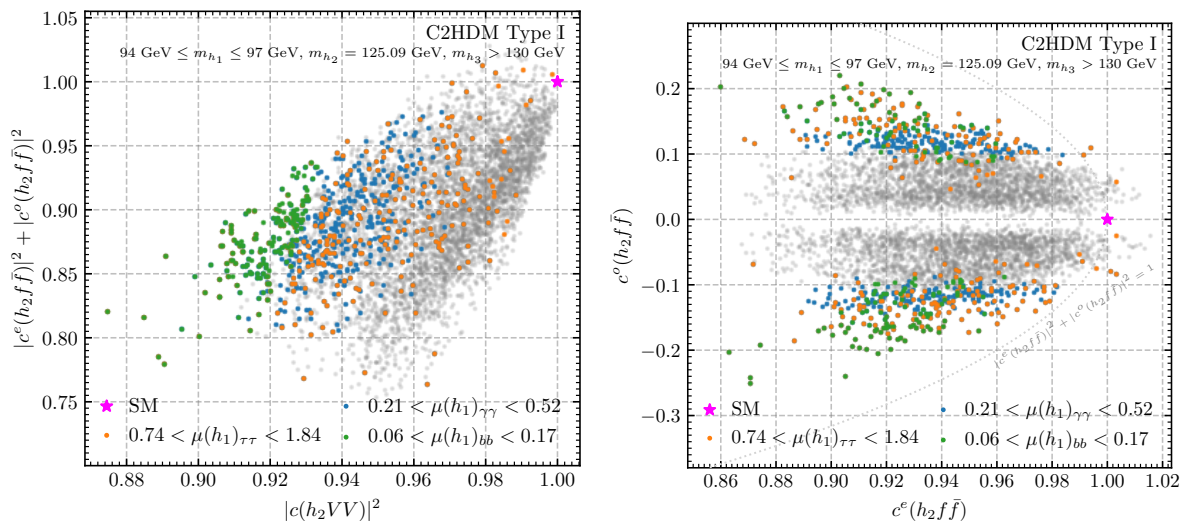


Figure 9: Coupling coefficients of $h_2 = h_{125}$ to gauge bosons and fermions. On the left, the squared coupling of h to fermions (including both CP-even and CP-odd contributions) vs. the respective squared coupling to gauge bosons is shown. On the right, the CP-odd contribution to the fermion coupling of h_2 c^o against the CP-even contribution to the same coupling, c^e , is shown. The dotted line indicates a Higgs coupling to fermions with magnitude identical to the SM. Blue, orange and green points predict a signal rate for the diphoton, ditau and LEP excess within the experimentally observed 1σ uncertainty bands, respectively (see Tab. 2). Green points are plotted on top of blue ones, which are coupled plotted on top of orange points. The remaining points are shown in grey. The SM prediction for the couplings coefficients is indicated with a magenta star.

proposed C2HDM scenario. In particular, assuming that the couplings of the state at 95 GeV are not measured precisely, probing the couplings of the SM-like Higgs boson might provide vital information about the possibility of distinguishing between different models that can describe the excesses.

In the left plot of Fig. 9, we show the squared coupling coefficients, i.e. κ -factors, for the couplings of h_{125} to gauge bosons on the horizontal axis and for the couplings to fermions on the vertical axis, where in the latter case we depict the squared sum of both the CP-even and the CP-odd component of the couplings. The predictions for the couplings of a SM Higgs boson are indicated with the magenta star, and the parameter points that fit the $b\bar{b}$ -excess, the diphoton-excess or the ditau-excess are indicated with the green, blue and orange points, respectively. According to the discussion above, demanding a description of the $b\bar{b}$ -excess observed at LEP gives rise to the largest deviations from the alignment limit and the SM predictions, with values of $|c(h_{125}VV)|^2 \lesssim 0.95$. For the parameter points fitting the diphoton excess, we find deviations from the SM of only a few percent in the squared coupling coefficients, and the ditau-excess can be described with deviations of only one percent.¹² These deviations are smaller than the expected experimental sensitivity with which the couplings of h_{125} can be measured during the high-luminosity runs of the LHC. Thus, the expected precision of a future e^+e^- collider like the International Linear Collider (ILC) could significantly improve the prospects of probing the 2HDM interpretation of the excesses at 95 GeV, determining the values of the underlying model parameters, and also to distinguish it from other scenarios discussed in the literature.

In order to quantify the amount of CP-violation in the couplings of the detected Higgs boson at 125 GeV predicted by the parameter points describing the excesses, we depict in the right plot of Fig. 9 the CP-even components $c^e(h_{125}f\bar{f})$ and the CP-odd components $c^o(h_{125}f\bar{f})$ of the couplings to fermions on the horizontal and the vertical axis, respectively. The color coding of the points is the same as the one in the left plot of Fig. 9 discussed above. One can see that a description of the three excesses is possible with values of the CP-odd coupling component at the level of $c^o(h_{125}f\bar{f}) \approx 0.1$, corresponding to an effective CP mixing angle of $\phi_{\text{CP}} = \tan^{-1} c^o(h_{125}f\bar{f})/c^e(h_{125}f\bar{f}) \lesssim 12^\circ$, which is substantially below the current experimental sensitivity at the LHC [107, 108]. However, under certain assumptions, the CP-violating phases of the scalar potential of the C2HDM can also be probed indirectly by experimental measurements of electric dipole moments, which will be discussed in more detail in Sect. 4.5.4.

4.5.2 Properties of the other BSM states

In Fig. 10, we show the allowed masses for h_3 and H^\pm in the region of parameter space satisfying all of the constraints mentioned, as well as the cross sections for their main production mechanisms. We observe that both masses lie in the rough range between 140 GeV and 340 GeV, with cross sections between about 2.5 pb and 9 pb for gluon-gluon production of h_3 , and between 1 pb and 13 pb for top-bottom-associated production of the charged scalar. Overall, the prospects of probing the C2HDM scenario via searches for the heavier scalar states are very similar to the prospects of the R2HDM scenario discussed in Sect. 4.2.2. Future LHC searches for $H^\pm \rightarrow tb$ and $h_3 \rightarrow VV$ could potentially exclude the still viable mass interval of H^\pm and h_3 in the scenario under investigation. Again, we emphasize that results for these searches utilizing the full

¹²We note that the implementation of the C2HDM in the code `ScannerS` does not allow for continuously approaching the CP-conserving limit of the model. Therefore, all parameter points of our scan in the C2HDM will feature some amount of CP-violation. This is why we performed a dedicated scan in the R2HDM whose results are discussed in Sect. 4.2.

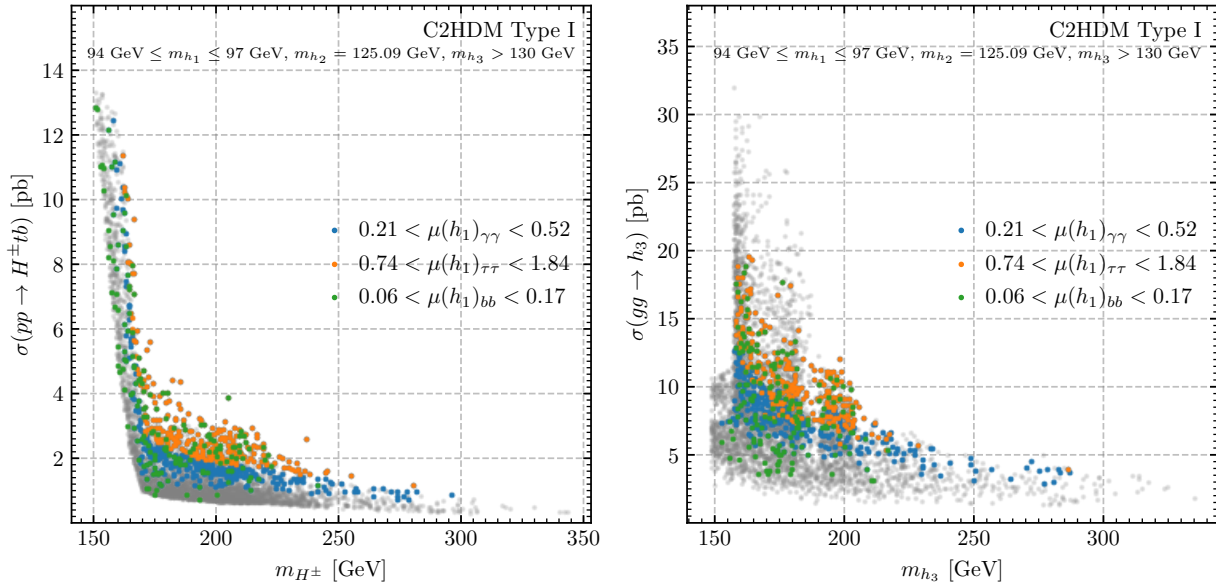


Figure 10: Allowed cross sections for h_3 and H^\pm production *vs* the respective masses. The blue, orange and green points describe the CMS diphoton excess, the CMS ditau excess or the LEP $b\bar{b}$ excess at the level of 1σ or better. The remaining points are shown in grey. All points satisfy the theoretical and experimental constraints considered previously, except for indirect constraints from flavour-physics observables and EDMs, which have not been applied here.

Run 2 dataset are so far only published for masses above 200 GeV. One overarching message we wish to convey, independently of the fate of the excesses, is the importance of covering also lower mass ranges in the experimental searches for new Higgs bosons, if possible.

4.5.3 Flavour-physics constraints

As in the R2HDM, the LHC diphoton and ditau can be accommodated within the Type-I C2HDM, with the added bonus that the LEP bottom excess can be fitted as well. Unlike the R2HDM, however, the region where two of these excesses are accommodated by the C2HDM is *not* necessarily in significant tension with flavour physics constraints. This much may be seen from Fig. 11, wherein we plot (in grey) all points from our scan in the $\tan\beta$ - m_{H^\pm} plane. Blue points denote the subset of points for which the LHC diphoton excess at 95 GeV are accommodated.¹³ We see that, unlike the case of the R2HDM, higher values of $\tan\beta$ are compatible with a description of the diphoton excess, and a sizeable number of points lie above the black dotted line and are thus allowed by the most stringent flavour physics constraints considered in Ref. [33], to wit limits on the $b \rightarrow s\gamma$ branching ratio. If one further attempts to describe the LHC ditau excess at 95 GeV, one is restricted to the parameter points shown in orange, which lie below the 2σ confidence-level exclusion line from flavour physics – this is due to the lower values of $\tan\beta$ required to accommodate this third signal, as had already been discussed in Fig. 7. However, a subset of orange points is above the dashed black line indicating the 3σ confidence-level exclusion limit from $b \rightarrow s\gamma$ measurements.

¹³The region where the LEP excess is described as well would not differ much from the region in which the blue points are located in Fig. 11, such that we do not highlight these points in the plot separately.

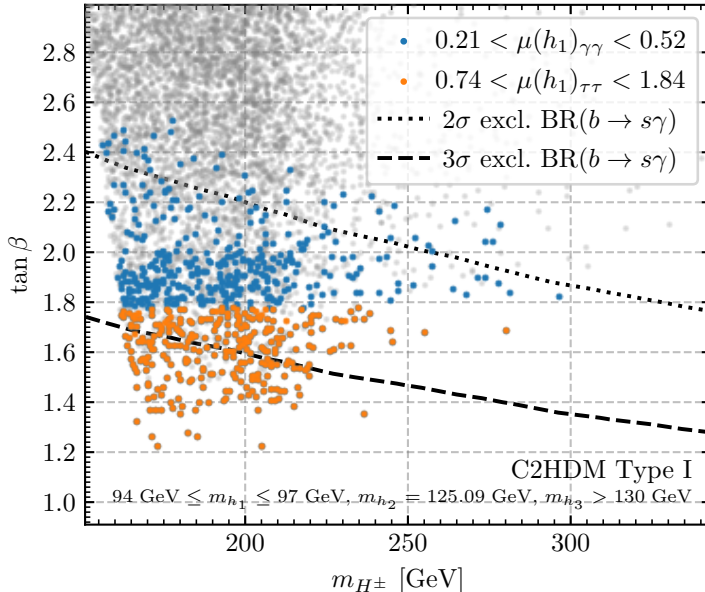


Figure 11: Flavour constraints in the $\tan\beta$ - m_{H^\pm} plane. Blue and orange points indicate the parameter points that describe the diphoton and the ditau excess at the level of 1σ or better, respectively, where orange points are plotted on top of blue points. The remaining parameter points are shown in grey. Parameter points fitting the LEP excess are not indicated here, since the corresponding signal rates are not strongly correlated with the values of $\tan\beta$ (see Fig. 7). The dotted and the dashed black lines indicate the exclusion limit from the measurements of $b \rightarrow s\gamma$ branching ratios at the 2σ and the 3σ confidence level, respectively, where the excluded regions are the parameter region below these lines.

4.5.4 EDM constraints

Given the new source of CP-violation in the scalar potential of the C2HDM, another way of probing the parameter points fitting the excesses is via potentially sizeable contributions to the static electric dipole moment (EDM) of fundamental particles. In particular for the electron, very precise measurements compatible with a vanishing EDM typically impose the strongest constraints on the parameter space of the C2HDM [109]. In order to confront the parameter space suitable for a description of the excesses at 95 GeV with these constraints, we use the prescription from Ref. [110] to compute the electron EDM and compare the theoretical predictions with the latest experimental upper limits at 90% confidence level published by the JILA Collaboration [111],

$$|d_e| < 4.1 \times 10^{-30} e \text{ cm} , \quad (4.32)$$

where e is the electric charge of the electron. In our parameter scan of the C2HDM, the maximum values obtained are of the order of $|d_e| \approx \mathcal{O}(10^{-27})$, with the bulk of points predicting an electron EDM at the level of $|d_e| \approx \mathcal{O}(10^{-28})$. Consequently, strictly applying the experimental upper limit from JILA would exclude all parameter points of our scan.

However, we stress that there are sizable theoretical uncertainties in the applications of these limits: the theory predictions are sensitive to the specifics of the UV completion of the 2HDM [106], even if the additional new physics lives at multi-TeV energy scales [112]. Moreover, focusing on the 2HDM particle content, large cancellations can be present between different contributions to the EDMs from the different scalars (for instance, if almost mass degenerate neutral scalar states are present [62]), and also additional sources of CP-violation in the Yukawa sector

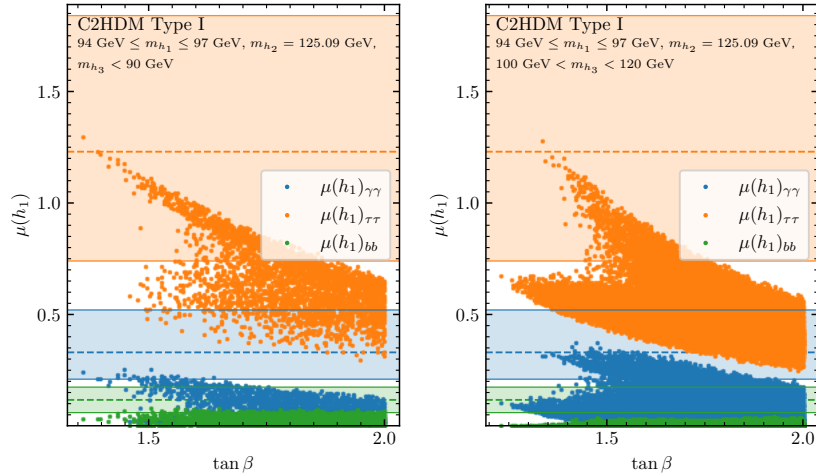


Figure 12: Signal rates for the diphoton, ditau and $b\bar{b}$ excesses *vs* $\tan\beta$ for a 95 GeV scalar within the Type I C2HDM and for different mass hierarchies. Except for constraints from flavour physics and EDMs, all theoretical and experimental constraints are applied. The bands correspond to the experimentally observed signal rates within their 1σ uncertainty band (see Tab. 2).

(not considered here) can play a role for the theory predictions of the EDMs (see e.g. Ref. [113] for a discussion in the general 2HDM). Since we want to remain agnostic about the UV completion of the 2HDM, and since we focus here on CP-violating effects only from the Higgs sector, whereas the EDMs also depend on the CP-phases in the fermion sector, we do not attempt a dedicated analysis with the goal of suppressing the electron EDM in order to be compatible with the limit from the JILA collaboration.

4.6 Complex 2HDM – $m_{h_1} = 95$ GeV, $m_{h_2} = 125$ GeV, $m_{h_3} < 120$ GeV

In the previous sections we considered the possibility of $h_{125} = h_2$ being the the second lightest neutral scalar. However, having a scalar $m_{h_3} < 120$ GeV is also allowed under the different theoretical and experimental cuts, in which case the detected Higgs boson at 125 GeV corresponds to the heaviest neutral scalar state. This mass hierarchy would imply that two neutral scalars below 125 GeV would have escaped detection so far, and we present those scenarios here for completeness. The results from our scans are shown in Fig. 12, for the two ranges $m_{h_3} < 90$ GeV and $100 \text{ GeV} < m_{h_3} < 120$ GeV, arising from the condition of not having mass degenerate states. The left plot shows that if $m_{h_3} < 90$ GeV, and the state h_1 at about 95 GeV is the second lightest of the three neutral scalars, a fit of the three signals – diphoton, ditau, LEP $b\bar{b}$ – is barely possible for $1.0 \lesssim \tan\beta \lesssim 1.7$. However, notice that the fit to the diphoton excess is very difficult to achieve in this scenario, with predicted signal rates at the lower end of the 1σ region. The plot on the right shows that, for the intermediate mass hierarchy, $100 \leq m_{h_3} \leq 120$ GeV, fitting the LEP signal is not possible, but the diphoton and ditau excesses may be fitted for $1.35 \lesssim \tan\beta \lesssim 1.75$.

In Fig. 13 we again show the correlation between the several μ -values, where it is easy to appreciate that the a sufficiently large diphoton signal is very difficult to accomplish for $m_{h_3} \leq 90$ GeV; and that the LEP fit cannot be accomplished if $100 \text{ GeV} \leq m_{h_3} \leq 120$ GeV. These light- h_3 scenarios are, therefore, less interesting than the situation considered in the previous sections, where h_3 is the heavier of the neutral scalars. For completeness, as with the first mass hierarchy studied, the points fulfilling both the ditau and diphoton excesses are at

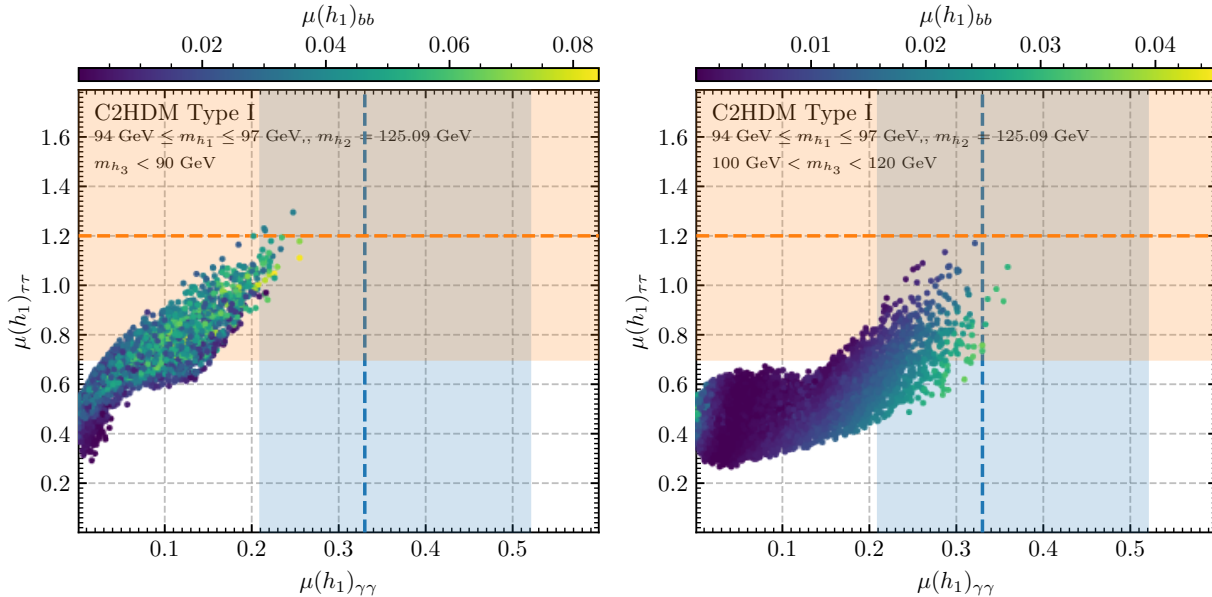


Figure 13: Diphoton signal rate *vs* ditau signal rate for a 95 GeV scalar within the Type I C2HDM. Except for constraints from flavour physics and EDMs, all theoretical and experimental constraints are applied. The bands correspond to the experimentally observed signal rates within their 1σ uncertainty band (see Tab. 2).

most between the 2σ and 3σ line of the $b \rightarrow s\gamma$ measurement.

4.7 Complex 2HDM – Lepton-specific

As a final note, we also investigated the Lepton-specific version of the C2HDM. Therein, the generated points are within the region $\tan\beta < 1$ and $m_{H^\pm} < 200$ GeV, such that points that can fulfill the signal ranges for the diphoton and ditau final states are in strong tension with flavour constraints at more than 3σ (*c.f.* Fig. 11). Therefore, we consider this scenario as excluded by current experimental data and will not discuss it in detail here.

5 Conclusions

The idea that there might be lighter scalars than the Higgs boson discovered at LHC in 2012 is quite enticing and it is not at all excluded by current experimental measurements. On the contrary, as the LHC accumulates data and searches for BSM particles become more refined, several interesting possibilities arose. Searches for diphoton decays at CMS have, since 2018, consistently indicated a (less than 3σ) excess for an invariant mass of 95 GeV. A possible ditau excess at a compatible mass is also observed by CMS, and, of course, that mass value reminds us of the presumed $b\bar{b}$ excess seemingly observed in the final days of LEP.

To interpret these possible signals as a spin-0 particle it would be desirable to have a “natural” mechanism to explain why a lighter scalar would only now be discovered, after the heavier SM-like 125 GeV Higgs boson discovery. The 2HDM provides a simple explanation for that – a CP-even 95 GeV scalar would have its couplings to electroweak gauge bosons suppressed due to the SM-like behaviour of the 125 GeV scalar; and a pseudoscalar of the same mass would not have been observed at LEP (thus the LEP anomaly would have been simply an experimental fluctuation) but could provide a nice explanation to the current LHC excesses at 95 GeV.

Flavour physics then dictates that, out of the different flavour-preserving versions of the 2HDM, models Type II or Flipped are ruled out, since $b \rightarrow s\gamma$ bounds impose a charged mass of several hundreds of GeV, and it becomes impossible to accommodate (due to unitarity constraints, as well as electroweak precision bounds) a lighter, 95 GeV, neutral state.

Our analysis shows that within the framework of the CP-conserving Type I 2HDM (R2HDM), a CP-even scalar with mass of 95 GeV could not fit both the ditau and diphoton data, unless very small values of $\tan\beta$ – highly disfavoured by flavour constraints – would be taken into account. On the contrary, assuming a pseudoscalar with mass 95 GeV, the higher production cross sections for such a particle (compared with a CP-even scalar of the same mass) allow for a simultaneous fit of both diphoton and ditau signals, though the LEP excess could not be fitted in this scenario. Unlike other attempts to fit these signals in the framework of the 2HDM, within the scenario proposed here, the only production mechanism required is gluon-gluon fusion. The resulting masses for the heavier CP-even scalar H and the charged Higgs H^\pm are relatively light (between roughly 160 and 250 GeV), and production cross sections for these BSM states are predicted by the model to range from 2 to 15 pb. The model will be, therefore, probed at Run 3 of the LHC, and we have shown that (again unlike other attempted theoretical explanations for these results) a fit of both diphoton and ditau data is possible even with minimal deviations from the alignment limit. There is, however, a problem with this scenario – $b \rightarrow s\gamma$ constraints disfavour, at 2.5σ or more, the range of charged masses and $\tan\beta$ required to fit both LHC excesses.

We were, in turn, led to the C2HDM, where CP violation in the potential is introduced via a soft \mathbb{Z}_2 -breaking term. The model has more freedom than the R2HDM to be in agreement with current experimental constraints. Within this more general framework, we find a fit to the three excesses – LHC diphoton and ditau, LEP $b\bar{b}$ – is possible for larger values of $\tan\beta$. Indeed, it even becomes possible to fit the diphoton and LEP signals (not the ditau one) so that the tension with $b \rightarrow s\gamma$ is now inferior to 2σ . With CP violation induced by the scalar potential, however, other bounds, such as those arising from electron EDMs, need to be considered. A quick analysis indicates that the region of parameter space suitable for a good description of all three signals would be in conflict with electron EDM data. Once again, the fit prefers masses for the charged and third neutral scalar below roughly 250 GeV and predicts sizeable production cross sections for those particles at the LHC.

Recently, the ATLAS collaboration has reported the full Run 2 results for searches for low-mass Higgs bosons in the di-photon final state. The model-dependent ATLAS analysis has a very similar sensitivity to the CMS search, showing the most significant excess over the SM background at a mass of about 95 GeV, consistent with the CMS di-photon excess. However, the excess observed by ATLAS is much less pronounced, such that a combination between CMS and ATLAS would yield slightly smaller signal rates for a possible state at 95 GeV. We have checked that combining the latest ATLAS diphoton search would not change the previous statements qualitatively: the three excesses can still be described simultaneously, although potentially with slightly larger $\tan\beta$ -values.

The remaining allowed mass interval for the charged Higgs bosons is found in the vicinity of the top-quark mass, where the LHC searches for $H^\pm \rightarrow tb$ lose sensitivity, but for which the exotic top-quark decay $t \rightarrow H^\pm b$ is still kinematically suppressed. In a similar fashion, assuming the mass hierarchy with h_{125} being the second lightest scalar state, the remaining allowed mass window for the third neutral scalar is found in the neighbourhood of twice the Z -boson mass. Larger values of $m_{h_3} \gtrsim 250$ GeV give rise to too large cross sections for the signature $pp \rightarrow h_3 \rightarrow h_1 Z$ with $h_1 = h_{95}$, which was searched for at the LHC assuming that h_1

decays in tau-lepton or bottom-quark pairs. On the other hand, values of $m_{h_3} \lesssim 160$ GeV are in tension with cross-section limits from LHC searches for $h_3 \rightarrow \tau^+\tau^-$. An overarching result of our study is that, independently of the fate of the excesses, LHC searches for rather light Higgs bosons at or around the EW scale still have significant potential to probe so far allowed parameter space regions of the 2HDM, in particular searches for Higgs bosons decaying into gauge bosons with masses below 200 GeV.

Further analysis of these possibilities for the Lepton-specific model, and for mass hierarchies with two scalars lighter than 120 GeV, reveals some interesting possibilities, but added tension with flavour constraints.

Clearly the preferred charged scalar mass and $\tan\beta$ region necessary for fitting the three excesses has tension with existing flavour sector results. Here it should be noted that these tensions would be somewhat weaker assuming a slightly smaller diphoton signal rate as suggested by the recent ATLAS search utilizing the full Run 2 dataset. We argue, though, that the tensions with data from flavour physics are not sufficient to invalidate this proposed solution for the LHC and LEP excesses at masses about 95 GeV. If the LHC excesses are confirmed by Run 3 data and still explainable by the 2HDM scenarios herein proposed, and tension with B-physics results persist, that could indicate, rather than the exclusion of the 2HDM, the need for a more complex flavour sector, with hitherto undiscovered BSM physics.

In short, we proposed several very economic theoretical frameworks for reproducing the CMS diphoton and ditau and the LEP $b\bar{b}$ excesses – so economical that, within the context of the R2HDM with a pseudoscalar of mass 95 GeV, the analysis can almost be made analytically. Confirmation of the excesses observed at the LHC by the Run 3 measurements is paramount. Reduced signal strengths for the diphoton and ditau signals would allow for larger values of $\tan\beta$ and weaken tensions with flavour physics constraints. Regardless, the explanations for the 95 GeV results within a 2HDM framework put forth in this work will be tested in Run 3 and will be easily disproven – or confirmed.¹⁴

Acknowledgements

The authors thank Georg Weiglein for bringing Ref. [76] to our attention. T.B. thanks Daniel Winterbottom for interesting discussions. P.M.F. is supported by *Fundação para a Ciência e a Tecnologia* (FCT) through contracts UIDB/00618/2020, UIDP/00618/2020, CERN/FIS-PAR/0004/2019, CERN/FIS-PAR/0014/2019 and CERN/FIS-PAR/0025/2021. The work of T.B. is supported by the German Bundesministerium für Bildung und Forschung (BMBF, Federal Ministry of Education and Research) – project 05H21VKCCA. D.A. is supported by the Deutsche Forschungsgemeinschaft (DFG, German Research Foundation) under grant 396021762 - TRR 257.

References

- [1] CMS collaboration, *Observation of a new boson at a mass of 125 GeV with the CMS experiment at the LHC*, *Phys. Lett.* **B716** (2012) 30 [[1207.7235](#)].
- [2] ATLAS collaboration, *Observation of a new particle in the search for the Standard Model Higgs boson with the ATLAS detector at the LHC*, *Phys. Lett.* **B716** (2012) 1 [[1207.7214](#)].

¹⁴Considering the authors' names, if the 95 GeV excesses discussed in this paper are experimentally confirmed and proven to be described by a 2HDM scalar, we propose that it be named the ABF, or even better, the FABulous particle.

- [3] CMS collaboration, *Search for a standard model-like Higgs boson in the mass range between 70 and 110 GeV in the diphoton final state in proton-proton collisions at $\sqrt{s} = 8$ and 13 TeV*, *Phys. Lett. B* **793** (2019) 320 [[1811.08459](#)].
- [4] CMS collaboration, *Search for low mass resonances in the diphoton final state in proton-proton collisions at $\sqrt{s} = 13$ TeV with the full Run 2 dataset*, Tech. Rep. [CMS-HIG-20-002](#) (2023).
- [5] S. Gascon-Shotkin, CMS, *Talk at MoriondEW: Searches for additional Higgs bosons at low mass*, [indico.cern.ch](#), 2023.
- [6] CMS collaboration, *Searches for additional Higgs bosons and for vector leptoquarks in $\tau\tau$ final states in proton-proton collisions at $\sqrt{s} = 13$ TeV*, [2208.02717](#).
- [7] LEP WORKING GROUP FOR HIGGS BOSON SEARCHES, ALEPH, DELPHI, L3, OPAL collaboration, *Search for the standard model Higgs boson at LEP*, *Phys. Lett. B* **565** (2003) 61 [[hep-ex/0306033](#)].
- [8] J. Cao, X. Guo, Y. He, P. Wu and Y. Zhang, *Diphoton signal of the light Higgs boson in natural NMSSM*, *Phys. Rev. D* **95** (2017) 116001 [[1612.08522](#)].
- [9] P.J. Fox and N. Weiner, *Light Signals from a Lighter Higgs*, *JHEP* **08** (2018) 025 [[1710.07649](#)].
- [10] U. Haisch and A. Malinauskas, *Let there be light from a second light Higgs doublet*, *JHEP* **03** (2018) 135 [[1712.06599](#)].
- [11] T. Biekötter, S. Heinemeyer and C. Muñoz, *Precise prediction for the Higgs-boson masses in the $\mu\nu$ SSM*, *Eur. Phys. J. C* **78** (2018) 504 [[1712.07475](#)].
- [12] D. Liu, J. Liu, C.E.M. Wagner and X.-P. Wang, *A Light Higgs at the LHC and the B-Anomalies*, *JHEP* **06** (2018) 150 [[1805.01476](#)].
- [13] F. Domingo, S. Heinemeyer, S. Paßehr and G. Weiglein, *Decays of the neutral Higgs bosons into SM fermions and gauge bosons in the CP-violating NMSSM*, *Eur. Phys. J. C* **78** (2018) 942 [[1807.06322](#)].
- [14] J.M. Cline and T. Toma, *Pseudo-Goldstone dark matter confronts cosmic ray and collider anomalies*, *Phys. Rev. D* **100** (2019) 035023 [[1906.02175](#)].
- [15] T. Biekötter, M. Chakraborti and S. Heinemeyer, *A 96 GeV Higgs boson in the N2HDM*, *Eur. Phys. J. C* **80** (2020) 2 [[1903.11661](#)].
- [16] J. Cao, X. Jia, Y. Yue, H. Zhou and P. Zhu, *96 GeV diphoton excess in seesaw extensions of the natural NMSSM*, *Phys. Rev. D* **101** (2020) 055008 [[1908.07206](#)].
- [17] T. Biekötter, S. Heinemeyer and G. Weiglein, *Mounting evidence for a 95 GeV Higgs boson*, *JHEP* **08** (2022) 201 [[2203.13180](#)].
- [18] T. Biekötter, S. Heinemeyer and G. Weiglein, *Excesses in the low-mass Higgs-boson search and the W-boson mass measurement*, *Eur. Phys. J. C* **83** (2022) 450 [[2204.05975](#)].
- [19] S. Iguro, T. Kitahara and Y. Omura, *Scrutinizing the 95–100 GeV di-tau excess in the top associated process*, *Eur. Phys. J. C* **82** (2022) 1053 [[2205.03187](#)].
- [20] S. Iguro, T. Kitahara, Y. Omura and H. Zhang, *Chasing the two-Higgs doublet model in the di-Higgs boson production*, *Phys. Rev. D* **107** (2023) 075017 [[2211.00011](#)].
- [21] T. Biekötter, S. Heinemeyer and G. Weiglein, *The CMS di-photon excess at 95 GeV in view of the LHC Run 2 results*, [2303.12018](#).
- [22] T. Biekötter, *Scalar extensions of the SM and recent experimental anomalies*, in *57th Rencontres de Moriond on Electroweak Interactions and Unified Theories*, 4, 2023 [[2304.11439](#)].
- [23] C. Bonilla, A.E. Cárcamo Hernández, S. Kovalenko, H. Lee, R. Pasechnik and I. Schmidt, *Fermion mass hierarchy in an extended left-right symmetric model*, [2305.11967](#).
- [24] ATLAS collaboration, *Search for diphoton resonances in the 66 to 110 GeV mass range using 140 fb⁻¹ of 13 TeV pp collisions collected with the ATLAS detector*, Tech. Rep. [ATLAS-CONF-2023-035](#), CERN, Geneva (2023).
- [25] T.D. Lee, *A Theory of Spontaneous T Violation*, *Phys. Rev.* **D8** (1973) 1226.
- [26] H. Haber and G. Kane, *The search for supersymmetry: Probing physics beyond the standard model*, *Physics Reports* **117** (1985) 75.
- [27] J.E. Kim, *Light Pseudoscalars*, *Particle Physics and Cosmology*, *Phys. Rept.* **150** (1987) 1.

- [28] R.D. Peccei and H.R. Quinn, *CP conservation in the presence of pseudoparticles*, *Phys. Rev. Lett.* **38** (1977) 1440.
- [29] G.C. Branco, P.M. Ferreira, L. Lavoura, M.N. Rebelo, M. Sher and J.a.P. Silva, *Theory and phenomenology of two-Higgs-doublet models*, *Phys. Rept.* **516** (2012) 1 [[1106.0034](#)].
- [30] S. Davidson and H.E. Haber, *Basis-independent methods for the two-Higgs-doublet model*, *Phys. Rev. D* **72** (2005) 035004 [[hep-ph/0504050](#)].
- [31] S.L. Glashow and S. Weinberg, *Natural Conservation Laws for Neutral Currents*, *Phys. Rev.* **D15** (1977) 1958.
- [32] E.A. Paschos, *Diagonal Neutral Currents*, *Phys. Rev.* **D15** (1977) 1966.
- [33] A. Arbey, F. Mahmoudi, O. Stal and T. Stefaniak, *Status of the Charged Higgs Boson in Two Higgs Doublet Models*, *Eur. Phys. J. C* **78** (2018) 182 [[1706.07414](#)].
- [34] T. Enomoto and R. Watanabe, *Flavor constraints on the Two Higgs Doublet Models of Z_2 symmetric and aligned types*, *JHEP* **05** (2016) 002 [[1511.05066](#)].
- [35] J.F. Gunion and H.E. Haber, *The CP conserving two Higgs doublet model: The Approach to the decoupling limit*, *Phys. Rev. D* **67** (2003) 075019 [[hep-ph/0207010](#)].
- [36] I.F. Ginzburg, M. Krawczyk and P. Osland, *Two Higgs doublet models with CP violation*, in *International Workshop on Linear Colliders (LCWS 2002)*, pp. 703–706, 11, 2002 [[hep-ph/0211371](#)].
- [37] W. Khater and P. Osland, *CP violation in top quark production at the LHC and two Higgs doublet models*, *Nucl. Phys. B* **661** (2003) 209 [[hep-ph/0302004](#)].
- [38] A.W. El Kaffas, W. Khater, O.M. Ogreid and P. Osland, *Consistency of the two Higgs doublet model and CP violation in top production at the LHC*, *Nucl. Phys.* **B775** (2007) 45 [[hep-ph/0605142](#)].
- [39] A.W. El Kaffas, P. Osland and O.M. Ogreid, *CP violation, stability and unitarity of the two Higgs doublet model*, *Nonlin. Phenom. Complex Syst.* **10** (2007) 347 [[hep-ph/0702097](#)].
- [40] A. Wahab El Kaffas, P. Osland and O.M. Ogreid, *Constraining the Two-Higgs-Doublet-Model parameter space*, *Phys. Rev.* **D76** (2007) 095001 [[0706.2997](#)].
- [41] P. Osland, P.N. Pandita and L. Selbuz, *Trilinear Higgs couplings in the two Higgs doublet model with CP violation*, *Phys. Rev. D* **78** (2008) 015003 [[0802.0060](#)].
- [42] B. Grzadkowski and P. Osland, *Tempered Two-Higgs-Doublet Model*, *Phys. Rev. D* **82** (2010) 125026 [[0910.4068](#)].
- [43] A. Arhrib, E. Christova, H. Eberl and E. Ginina, *CP violation in charged Higgs production and decays in the Complex Two Higgs Doublet Model*, *JHEP* **04** (2011) 089 [[1011.6560](#)].
- [44] A. Barroso, P.M. Ferreira, R. Santos and J.P. Silva, *Probing the scalar-pseudoscalar mixing in the 125 GeV Higgs particle with current data*, *Phys. Rev. D* **86** (2012) 015022 [[1205.4247](#)].
- [45] Y.B. Zeldovich, I.Y. Kobzarev and L.B. Okun, *Cosmological Consequences of the Spontaneous Breakdown of Discrete Symmetry*, *Zh. Eksp. Teor. Fiz.* **67** (1974) 3.
- [46] N.G. Deshpande and E. Ma, *Pattern of Symmetry Breaking with Two Higgs Doublets*, *Phys.Rev.* **D18** (1978) 2574.
- [47] I.P. Ivanov, *Minkowski space structure of the Higgs potential in 2HDM*, *Phys. Rev.* **D75** (2007) 035001 [[hep-ph/0609018](#)].
- [48] I.P. Ivanov, *Minkowski space structure of the Higgs potential in 2HDM. II. Minima, symmetries, and topology*, *Phys. Rev.* **D77** (2008) 015017 [[0710.3490](#)].
- [49] S. Kanemura and K. Yagyu, *Unitarity bound in the most general two Higgs doublet model*, *Phys. Lett. B* **751** (2015) 289 [[1509.06060](#)].
- [50] I.F. Ginzburg and I.P. Ivanov, *Tree-level unitarity constraints in the most general 2HDM*, *Phys. Rev. D* **72** (2005) 115010 [[hep-ph/0508020](#)].
- [51] H.E. Haber and D. O’Neil, *Basis-independent methods for the two-Higgs-doublet model III: The CP-conserving limit, custodial symmetry, and the oblique parameters S , T , U* , *Phys. Rev. D* **83** (2011) 055017 [[1011.6188](#)].

- [52] M. Mühlleitner, M.O.P. Sampaio, R. Santos and J. Wittbrodt, *ScannerS: parameter scans in extended scalar sectors*, *Eur. Phys. J. C* **82** (2022) 198 [2007.02985].
- [53] H. Bahl, T. Biekötter, S. Heinemeyer, C. Li, S. Paasch, G. Weiglein et al., *HiggsTools: BSM scalar phenomenology with new versions of HiggsBounds and HiggsSignals*, 2210.09332.
- [54] P. Bechtle, O. Brein, S. Heinemeyer, G. Weiglein and K.E. Williams, *HiggsBounds: Confronting Arbitrary Higgs Sectors with Exclusion Bounds from LEP and the Tevatron*, *Comput. Phys. Commun.* **181** (2010) 138 [0811.4169].
- [55] P. Bechtle, O. Brein, S. Heinemeyer, G. Weiglein and K.E. Williams, *HiggsBounds 2.0.0: Confronting Neutral and Charged Higgs Sector Predictions with Exclusion Bounds from LEP and the Tevatron*, *Comput. Phys. Commun.* **182** (2011) 2605 [1102.1898].
- [56] P. Bechtle, O. Brein, S. Heinemeyer, O. Stål, T. Stefaniak, G. Weiglein et al., *HiggsBounds – 4: Improved Tests of Extended Higgs Sectors against Exclusion Bounds from LEP, the Tevatron and the LHC*, *Eur. Phys. J. C* **74** (2014) 2693 [1311.0055].
- [57] P. Bechtle, D. Dercks, S. Heinemeyer, T. Klingl, T. Stefaniak, G. Weiglein et al., *HiggsBounds-5: Testing Higgs Sectors in the LHC 13 TeV Era*, *Eur. Phys. J. C* **80** (2020) 1211 [2006.06007].
- [58] P. Bechtle, S. Heinemeyer, O. Stål, T. Stefaniak and G. Weiglein, *HiggsSignals: Confronting arbitrary Higgs sectors with measurements at the Tevatron and the LHC*, *Eur. Phys. J. C* **74** (2014) 2711 [1305.1933].
- [59] P. Bechtle, S. Heinemeyer, O. Stål, T. Stefaniak and G. Weiglein, *Probing the Standard Model with Higgs signal rates from the Tevatron, the LHC and a future ILC*, *JHEP* **11** (2014) 039 [1403.1582].
- [60] P. Bechtle, S. Heinemeyer, T. Klingl, T. Stefaniak, G. Weiglein and J. Wittbrodt, *HiggsSignals-2: Probing new physics with precision Higgs measurements in the LHC 13 TeV era*, *Eur. Phys. J. C* **81** (2021) 145 [2012.09197].
- [61] M. Mühlleitner, M.O.P. Sampaio, R. Santos and J. Wittbrodt, *Phenomenological Comparison of Models with Extended Higgs Sectors*, *JHEP* **08** (2017) 132 [1703.07750].
- [62] D. Fontes, J.C. Romão and J.a.P. Silva, *$h \rightarrow Z\gamma$ in the complex two Higgs doublet model*, *JHEP* **12** (2014) 043 [1408.2534].
- [63] CMS collaboration, *Search for new resonances in the diphoton final state in the mass range between 80 and 110 GeV in pp collisions at $\sqrt{s} = 8$ TeV*, Tech. Rep. CMS-PAS-HIG-14-037 (2015).
- [64] ATLAS collaboration, *Search for resonances in the 65 to 110 GeV diphoton invariant mass range using 80 fb⁻¹ of pp collisions collected at $\sqrt{s} = 13$ TeV with the ATLAS detector*, Tech. Rep. ATLAS-CONF-2018-025 (7, 2018).
- [65] CMS collaboration, *Search for dilepton resonances from decays of (pseudo)scalar bosons produced in association with a massive vector boson or top quark anti-top quark pair at $\sqrt{s} = 13$ TeV*, Tech. Rep. CMS-PAS-EXO-21-018 (2022).
- [66] LEP WORKING GROUP FOR HIGGS BOSON SEARCHES, ALEPH, DELPHI, L3, OPAL collaboration, *Search for the standard model Higgs boson at LEP*, *Phys. Lett. B* **565** (2003) 61 [hep-ex/0306033].
- [67] ALEPH, DELPHI, L3, OPAL, LEP WORKING GROUP FOR HIGGS BOSON SEARCHES collaboration, *Search for neutral MSSM Higgs bosons at LEP*, *Eur. Phys. J. C* **47** (2006) 547 [hep-ex/0602042].
- [68] T. Biekötter and M. Pierre, *Higgs-boson visible and invisible constraints on hidden sectors*, *Eur. Phys. J. C* **82** (2022) 1026 [2208.05505].
- [69] ATLAS collaboration, *Combined measurements of Higgs boson production and decay using up to 139 fb⁻¹ of proton-proton collision data at $\sqrt{s} = 13$ TeV collected with the ATLAS experiment*, Tech. Rep. ATLAS-CONF-2021-053, CERN, Geneva (2021).
- [70] T. Biekötter and M.O. Olea-Romacho, *Reconciling Higgs physics and pseudo-Nambu-Goldstone dark matter in the S2HDM using a genetic algorithm*, *JHEP* **10** (2021) 215 [2108.10864].
- [71] S. Heinemeyer, C. Li, F. Lika, G. Moortgat-Pick and S. Paasch, *Phenomenology of a 96 GeV Higgs boson in the 2HDM with an additional singlet*, *Phys. Rev. D* **106** (2022) 075003 [2112.11958].
- [72] CDF collaboration, *High-precision measurement of the W boson mass with the CDF II detector*, *Science* **376** (2022) 170.

- [73] CMS collaboration, *Search for a new resonance decaying to two scalars in the final state with two bottom quarks and two photons in proton-proton collisions at $\sqrt{s} = 13$ TeV*, Tech. Rep. [CMS-PAS-HIG-21-011](#), CERN, Geneva (2022).
- [74] CMS collaboration, *Search for a heavy Higgs boson decaying into two lighter Higgs bosons in the $\tau\tau b\bar{b}$ final state at 13 TeV*, *JHEP* **11** (2021) 057 [[2106.10361](#)].
- [75] S. Banik, A. Crivellin, S. Iguro and T. Kitahara, *Asymmetric Di-Higgs Signals of the N2HDM-U(1)*, [2303.11351](#).
- [76] ATLAS collaboration, *Anomaly detection search for new resonances decaying into a Higgs boson and a generic new particle X in hadronic final states using $\sqrt{s} = 13$ TeV pp collisions with the ATLAS detector*, [2306.03637](#).
- [77] G. Coloretti, A. Crivellin, S. Bhattacharya and B. Mellado, *Searching for Low-Mass Resonances Decaying into W Bosons*, [2302.07276](#).
- [78] CMS collaboration, *Measurements of the Higgs boson production cross section and couplings in the W boson pair decay channel in proton-proton collisions at $\sqrt{s} = 13$ TeV*, [2206.09466](#).
- [79] ATLAS collaboration, *Measurements of Higgs boson production by gluon–gluon fusion and vector-boson fusion using $H \rightarrow WW^* \rightarrow e\nu\mu\nu$ decays in pp collisions at $\sqrt{s} = 13$ TeV with the ATLAS detector*, [2207.00338](#).
- [80] A. Barroso, P. Ferreira, I. Ivanov and R. Santos, *Metastability bounds on the two Higgs doublet model*, *JHEP* **06** (2013) 045 [[1303.5098](#)].
- [81] I. Ivanov and J.a.P. Silva, *Tree-level metastability bounds for the most general two Higgs doublet model*, *Phys. Rev. D* **92** (2015) 055017 [[1507.05100](#)].
- [82] T. Biekötter, S. Heinemeyer, J.M. No, M.O. Olea-Romacho and G. Weiglein, *The trap in the early Universe: impact on the interplay between gravitational waves and LHC physics in the 2HDM*, *JCAP* **03** (2023) 031 [[2208.14466](#)].
- [83] GFITTER GROUP collaboration, *The global electroweak fit at NNLO and prospects for the LHC and ILC*, *Eur. Phys. J. C* **74** (2014) 3046 [[1407.3792](#)].
- [84] W. Grimus, L. Lavoura, O.M. Ogreid and P. Osland, *A Precision constraint on multi-Higgs-doublet models*, *J. Phys. G* **35** (2008) 075001 [[0711.4022](#)].
- [85] ATLAS, CMS collaboration, *Combined Measurement of the Higgs Boson Mass in pp Collisions at $\sqrt{s} = 7$ and 8 TeV with the ATLAS and CMS Experiments*, *Phys. Rev. Lett.* **114** (2015) 191803 [[1503.07589](#)].
- [86] O. Deschamps, S. Descotes-Genon, S. Monteil, V. Niess, S. T’Jampens and V. Tisserand, *The Two Higgs Doublet of Type II facing flavour physics data*, *Phys. Rev. D* **82** (2010) 073012 [[0907.5135](#)].
- [87] F. Mahmoudi and O. Stal, *Flavor constraints on the two-Higgs-doublet model with general Yukawa couplings*, *Phys. Rev. D* **81** (2010) 035016 [[0907.1791](#)].
- [88] T. Hermann, M. Misiak and M. Steinhauser, *$\bar{B} \rightarrow X_s \gamma$ in the Two Higgs Doublet Model up to Next-to-Next-to-Leading Order in QCD*, *JHEP* **11** (2012) 036 [[1208.2788](#)].
- [89] M. Misiak et al., *Updated NNLO QCD predictions for the weak radiative B-meson decays*, *Phys. Rev. Lett.* **114** (2015) 221801 [[1503.01789](#)].
- [90] M. Misiak and M. Steinhauser, *Weak radiative decays of the B meson and bounds on M_{H^\pm} in the Two-Higgs-Doublet Model*, *Eur. Phys. J. C* **77** (2017) 201 [[1702.04571](#)].
- [91] M. Misiak, A. Rehman and M. Steinhauser, *Towards $\bar{B} \rightarrow X_s \gamma$ at the NNLO in QCD without interpolation in m_c* , *JHEP* **06** (2020) 175 [[2002.01548](#)].
- [92] LHC HIGGS CROSS SECTION WORKING GROUP collaboration, *Handbook of LHC Higgs Cross Sections: 4. Deciphering the Nature of the Higgs Sector*, [1610.07922](#).
- [93] A. Djouadi, J. Kalinowski and M. Spira, *HDECAY: A Program for Higgs boson decays in the standard model and its supersymmetric extension*, *Comput. Phys. Commun.* **108** (1998) 56 [[hep-ph/9704448](#)].
- [94] ATLAS collaboration, *Search for charged Higgs bosons decaying into a top quark and a bottom quark at $\sqrt{s} = 13$ TeV with the ATLAS detector*, *JHEP* **06** (2021) 145 [[2102.10076](#)].
- [95] CMS collaboration, *Search for charged Higgs bosons decaying into a top and a bottom quark in the all-jet final state of pp collisions at $\sqrt{s} = 13$ TeV*, *JHEP* **07** (2020) 126 [[2001.07763](#)].

- [96] H. Bahl, T. Stefaniak and J. Wittbrodt, *The forgotten channels: charged Higgs boson decays to a W and a non-SM-like Higgs boson*, *JHEP* **06** (2021) 183 [[2103.07484](#)].
- [97] ATLAS collaboration, *Search for charged Higgs bosons decaying via $H^\pm \rightarrow \tau^\pm \nu_\tau$ in the τ +jets and τ +lepton final states with 36 fb^{-1} of pp collision data recorded at $\sqrt{s} = 13 \text{ TeV}$ with the ATLAS experiment*, *JHEP* **09** (2018) 139 [[1807.07915](#)].
- [98] CMS collaboration, *Search for a new scalar resonance decaying to a pair of Z bosons in proton-proton collisions at $\sqrt{s} = 13 \text{ TeV}$* , *JHEP* **06** (2018) 127 [[1804.01939](#)].
- [99] CMS collaboration, *Search for neutral resonances decaying into a Z boson and a pair of b jets or τ leptons*, *Phys. Lett. B* **759** (2016) 369 [[1603.02991](#)].
- [100] CMS collaboration, *Search for new neutral Higgs bosons through the $H \rightarrow ZA \rightarrow \ell^+ \ell^- b \bar{b}$ process in pp collisions at $\sqrt{s} = 13 \text{ TeV}$* , *JHEP* **03** (2020) 055 [[1911.03781](#)].
- [101] ATLAS collaboration, *Search for heavy Higgs bosons decaying into two tau leptons with the ATLAS detector using pp collisions at $\sqrt{s} = 13 \text{ TeV}$* , *Phys. Rev. Lett.* **125** (2020) 051801 [[2002.12223](#)].
- [102] CMS collaboration, *Search for additional neutral MSSM Higgs bosons in the $\tau\tau$ final state in proton-proton collisions at $\sqrt{s} = 13 \text{ TeV}$* , *JHEP* **09** (2018) 007 [[1803.06553](#)].
- [103] F. Mahmoudi, *SuperIso: A Program for calculating the isospin asymmetry of $B \rightarrow K^* \gamma$ in the MSSM*, *Comput. Phys. Commun.* **178** (2008) 745 [[0710.2067](#)].
- [104] F. Mahmoudi, *SuperIso v2.3: A Program for calculating flavor physics observables in Supersymmetry*, *Comput. Phys. Commun.* **180** (2009) 1579 [[0808.3144](#)].
- [105] HEAVY FLAVOR AVERAGING GROUP, HFLAV collaboration, *Averages of b-hadron, c-hadron, and τ -lepton properties as of 2021*, *Phys. Rev. D* **107** (2023) 052008 [[2206.07501](#)].
- [106] M. Jung and A. Pich, *Electric Dipole Moments in Two-Higgs-Doublet Models*, *JHEP* **04** (2014) 076 [[1308.6283](#)].
- [107] CMS collaboration, *Analysis of the CP structure of the Yukawa coupling between the Higgs boson and τ leptons in proton-proton collisions at $\sqrt{s} = 13 \text{ TeV}$* , *JHEP* **06** (2022) 012 [[2110.04836](#)].
- [108] ATLAS collaboration, *Measurement of the CP properties of Higgs boson interactions with τ -leptons with the ATLAS detector*, [2212.05833](#).
- [109] D. Fontes, M. Mühlleitner, J.C. Romão, R. Santos, J.a.P. Silva and J. Wittbrodt, *The C2HDM revisited*, *JHEP* **02** (2018) 073 [[1711.09419](#)].
- [110] T. Abe, J. Hisano, T. Kitahara and K. Tobioka, *Gauge invariant Barr-Zee type contributions to fermionic EDMs in the two-Higgs doublet models*, *JHEP* **01** (2014) 106 [[1311.4704](#)].
- [111] T.S. Roussy et al., *A new bound on the electron's electric dipole moment*, [2212.11841](#).
- [112] C. Cesarotti, Q. Lu, Y. Nakai, A. Parikh and M. Reece, *Interpreting the Electron EDM Constraint*, *JHEP* **05** (2019) 059 [[1810.07736](#)].
- [113] K. Fuyuto, W.-S. Hou and E. Senaha, *Cancellation mechanism for the electron electric dipole moment connected with the baryon asymmetry of the Universe*, *Phys. Rev. D* **101** (2020) 011901 [[1910.12404](#)].